Identification of Putative Agouti-Related Protein(87−132)-Melanocortin-4 Receptor Interactions by Homology Molecular Modeling and Validation Using Chimeric Peptide Ligands

Andrzej Wilczynski,[#,†] Xiang S. Wang,[‡,†] Christine G. Joseph,[#] Zhimin Xiang,[#] Rayna M. Bauzo,[#] Joseph W. Scott,[#] Nicholas B. Sorensen,[#] Amanda M. Shaw,[§] William J. Millard,[§] Nigel G. Richards,[‡] and Carrie Haskell-Luevano*[,#]

Departments of Medicinal Chemistry, Chemistry, and Pharmacodynamics, University of Florida, Gainesville, Florida 32610

Received July 29, 2003

Agouti-related protein (AGRP) is one of only two naturally known antagonists of G-protein-coupled receptors (GPCRs) identified to date. Specifically, AGRP antagonizes the brain melanocortin-3 and -4 receptors involved in energy homeostasis. α-Melanocyte stimulating hormone (α-MSH) is one of the known endogenous agonists for these melanocortin receptors. Insight into putative interactions between the antagonist AGRP amino acids with the melanocortin-4 receptor (MC4R) may be important for the design of unique ligands for the treatment of obesity related diseases and is currently lacking in the literature. A three-dimensional homology molecular model of the mouse MC4 receptor complex with the hAGRP-(87−132) ligand docked into the receptor has been developed to identify putative antagonist ligand−receptor interactions. Key putative AGRP−MC4R interactions include the Arg111 of hAGRP(87−132) interacting in a negatively charged pocket located in a cavity formed by transmembrane spanning (TM) helices 1, 2, 3, and 7, capped by the acidic first extracellular loop (EL1) and specifically with the conserved melanocortin receptor residues mMC4R Glu92 (TM2), mMC4R Asp114 (TM3), and mMC4R Asp118 (TM3). Additionally, Phe112 and Phe113 of hAGRP(87−132) putatively interact with an aromatic hydrophobic pocket formed by the mMC4 receptor residues Phe176 (TM4), Phe193 (TM5), Phe253 (TM6), and Phe254 (TM6). To validate the AGRP−mMC4R model complex presented herein from a ligand perspective, we generated nine chimeric peptide ligands based on a modified antagonist template of the hAGRP-(109−118) (Tyr-c[Asp-Arg-Phe-Phe-Asn-Ala-Phe-Dpr]-Tyr-NH_2). In these chimeric ligands, the antagonist AGRP Arg-Phe-Phe residues were replaced by the melanocortin agonist His/D-Phe-Arg-Trp amino acids. These peptides resulted in agonist activity at the mouse melanocortin receptors (mMC1R and mMC3−5Rs). The most notable results include the identification of a novel subnanomolar melanocortin peptide template Tyr-c[Asp-His-DPhe-Arg-Trp-Asn-Ala-Phe-Dpr]-Tyr-NH_2 that is equipotent to α-MSH at the mMC1, mMC3, and mMC5 receptors but is 30-fold more potent than α-MSH at the mMC4R. Additionally, these studies identified a new and novel >200-fold MC4R versus MC3R selective peptide Tyr-c[Asp-D-Phe-Arg-Trp-Asn-Ala-Phe-Dpr]-Tyr-NH_2 template. Furthermore, when the His-DPhe-Arg-Trp sequence is used to replace the hAGRP Arg-Phe-Phe residues in the "mini"-AGRP (hAGRP87−120, C105A) template, a potent nanomolar agonist resulted at the mMC1R and MC3−5Rs.

Introduction

Agouti-related protein (AGRP) and the melanocortin-4 receptor (MC4R) have both been identified as directly regulating food intake, obesity, and energy homeostasis.[1,2] Both of these proteins are members of the melanocortin system that consists of five G-protein-coupled receptors (MC1−5R),[3−9] endogenous agonists derived from posttranslational modification of the proopiomelanocortin (POMC) gene transcript,[10] endogenous antagonists agouti[11] and agouti-related protein,[1] and auxiliary protein families (mahogany/attractin and syndecans)[12−15] that appear to regulate the function of the endogenous antagonists. Agouti and AGRP both function as competitive antagonists of endogenous melanocortin agonists at the melanocortin receptors, specifically, agouti antagonizes the MC1R, the MC4R, and possibly the MC3R (appears to be species-dependent),[11] while AGRP antagonizes the MC3 and MC4 receptors expressed in the brain.[1] Additionally, AGRP appears to function as an inverse agonist (in the absence of agonist ligand) at the MC4R.[16−18] Since the normal physiological role of agouti is regulation of skin pigmentation and animal coat coloration,[19] but the normal physiological role of AGRP appears to be involved in the regulation of energy homeostasis and obesity,[1] AGRP may be an important therapeutic target for both the understanding and treatment of obesity-related diseases. Surprisingly, very little is currently known about specific molecular interactions of AGRP with the melanocortin receptors, the mechanism(s) regulating food intake and obesity, and the molecular interactions with the auxiliary pro-

* To whom correspondence should be addressed. Phone: (352) 846-2722. Fax: (352) 392-8182. E-mail: Carrie@cop.ufl.edu.
[#] Department of Medicinal Chemistry.
[†] These authors contributed equally to this manuscript.
[‡] Department of Chemistry.
[§] Department of Pharmacodynamics.

10.1021/jm0303608 CCC: $27.50
Published on Web 03/20/2004

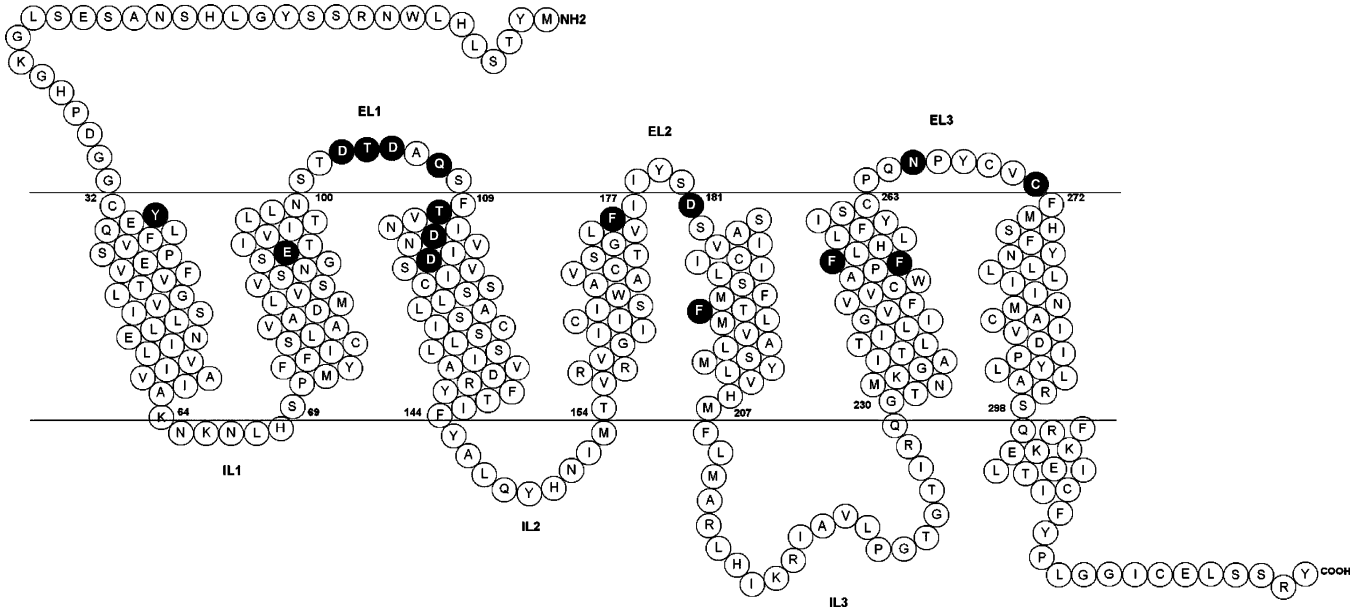

Figure 1. Schematic diagram of the mouse melanocortin 4-receptor. The horizontal black lines represent the approximate membrane boundaries. Black circles with white text indicate the amino acids involved in the putative AGRP(87−132)−mMC4R interactions. The Arabic numbers indicate the position of the residues inside the TM domain. EL = extracellular loop. IL = intracellular loop.

tein families (mahogany/attractin and syndecans) that appear to interact with AGRP upstream from the MC4R. In the study presented here, we attempt to identify specific putative hAGRP(87−132) interactions with the mouse MC4R using a three-dimensional homology molecular modeling strategy that we can validate by the design, synthesis, and pharmacological evaluation of chimeric antagonist hAGRP−melanocortin agonist ligands.

Results

Homology Molecular Modeling of the AGRP(87−132)-Mouse Melanocortin-4 Receptor. A two-dimensional serpentine representation of the mMC4R is presented in Figure 1 and Table 1, summarizing the MC4R residues identified that putatively interact with the hAGRP(87−132) antagonist ligand, based on three-dimensional homology molecular modeling presented herein and previously reported mutagenesis data.[20] The AGRP−mMC4R homology model complex (Figure 2) was generated using the G-protein-coupled receptor (GPCR) rhodopsin structure template[21] and the hAGRP-(87−132) structure based on NMR studies.[22]

For relatively large peptide ligands, in particular hAGRP(87−132), there is some evidence that the extracellular loops (ELs) contribute to molecular recognition and receptor functional activity.[23,24] In this study, our mMC4 receptor model has been extended beyond the transmembrane-spanning domains (TM) to include the intra- and extracellular loops. The loop PDB database search results and the GOR 4.0 secondary structure analysis results are summarized in Table 2. The overall architecture of the average-minimized mMC4 receptor structure, after simulated annealing, is shown in Figure 2A. The highly conserved melanocortin receptor EL1 loop, comprising acidic motif Asp-X-Asp, is arranged around the edge of the cavity formed by TM helices 1, 2, 3, and 7. This arrangement is particularly striking, since a putative binding pocket for both MC4R agonists and antagonists has already been postulated, which is located among TMs 1, 2, 3, 6, and 7.[24−28] Viewed from the top, this particular configuration of EL1 is potentially involved in the AGRP ligand interactions with the putative TM domain binding pocket. The second extracellular loop (EL2) spans the TM 4 and 5 helices. The EL3 loop forms a flat span between the ends of TM6 and TM7, without any specific folding pattern.

The refined averaged NMR structure of hAGRP(87−132)[29] docked into the mouse MC4 receptor is illustrated in Figure 2B−D. Table 1 summarizes putative hAGRP-(87−132) amino acid intermolecular interactions with the mMC4R and intramolecular interactions within hAGRP(87−132). Figure 3 summarizes the hAGRP-(111−113) Arg-Phe-Phe antagonist amino acids putatively interacting with the mMC4 receptor residues in the proposed overlapping "key" binding pocket with the critical D-Phe-Arg-Trp melanocortin agonist residues (Figure 4).[20,28] The hAGRP Arg111 amino acid putatively interacts with the mMC4R in a negatively charged pocket formed by the highly conserved melanocortin receptor residues Glu92 (TM2), Asp114 (TM3), and Asp118 (TM3) (Figures 2C and 3). The mMC4R acidic Glu/Asp side chains form a strong and stabilizing ionic bridge with the basic guanidinium moiety of the hAGRP Arg111 amino acid. These results are consistent with the experimental receptor mutagenesis data of both the human and mouse MC4R.[20,28] Point mutations of these highly conserved melanocortin residues Glu92Lys and Asp118Lys resulted in >1000-fold loss in binding affinity mutant mMC4Rs, suggesting that electrostatic interactions among these MC4R residues are important for melanocortin agonist and antagonist binding.[20] An electrostatic surface potential was calculated and displayed with the GRASP program[30] (data not shown), correlating interactions between the negative potential region corresponding to the formal negative charge of the mMC4R Glu92, Asp114, and Asp118 residues and positive surface of the hAGRP Arg111 amino acid.

Table 1. Putative hAGRP(87−132) Amino Acid Intramolecular and Intermolecular Interactions with the mMC4 Receptor[a]

hAGRP(87−132) amino acid	mMC4R−hAGRP residue
Arg89	hAGRPGlu92 backbone of Cys271 (EL3 adjacent to TM7 initiation)
His91	Thr104 (EL1) backbone C═O of Asp103 (EL1) Tyr33 (N-termini adjacent to TM1 initiation)
Glu92	hAGRPArg89
Ser93	backbone of Cys271 (EL3 adjacent to TM7 initiation)
Gln97	hAGRPAsn114 Asp181 (EL2 adjacent to TM5 initiation)
Gln98	Asn266 (EL3)
Tyr109	Asp114 (TM3)
Arg111	Glu92 (TM2) Asp114 (TM3) Asp118 (TM3)
Phe112	Phe176 (end of TM4 adjacent to EL2 initiation) Phe253 (TM6)
Phe113	Phe176 (end of TM4 adjacent to EL2 initiation) Phe193 (TM5) Phe253 (TM6) Phe254 (TM6)
Asn114	hAGRPGln97 Asp181 (EL2 adjacent to TM5 initiation)
Phe116	hAGRPTyr118
Tyr118	Asp105 (EL1) Gln107 (EL1) hAGRPPhe116
Arg120	Asp105 (EL1) Asp114 (TM3)
Lys121	hAGRPAsp103 Asp103 (EL1)
Thr124	Thr110 (end of EL1 adjacent to TM3 initiation)
Arg131	backbone of Ala106 (EL1)
Thr132	Thr104 (EL1)

[a] Unless otherwise noted, the putative ligand−receptor interactions are with the mMC4 receptor side chain to side chain.

A cluster of mMC4R aromatic and hydrophobic Phe residues within the putative ligand-binding cavity are created by amino acids located in TMs 4−6, illustrated in Figures 2D and 3. The Phe112 and Phe113 residues of hAGRP(87−132) are observed to putatively interact with this aromatic hydrophobic receptor pocket consisting of the mMC4R Phe176 (TM4), Phe193 (TM5), Phe253 (TM6), and Phe254 (TM6) residues. Experimental in vitro mutagenesis studies of the MC4R resulted in the identification of single-point mutations of the mMC4R Phe176, Phe193, and Phe254 amino acids to Ser or Lys residues, which resulted in decreased hAGRP-(87−132) binding affinity by 4- to 7-fold.[20] The mMC4R Phe253Ser modification in TM6 resulted in a >1000-fold decrease in binding, suggesting that the side chain and putatively the aromaticity at Phe253 as well as the Phe176, Phe193, and Phe254 receptor residues may be important for ligand−receptor interactions. The model presented herein provides "pseudo" molecular insight into these mutations. While the mMC4R Tyr179 at EL2 does not appear to directly contact the hAGRP Phe112 or Phe113 amino acids, its proximity to the aromatic pocket may infer indirect participation in stabilization of the aromatic cluster. The mMC4R Phe259 (TM6) is located above the aromatic binding pocket and does not appear to directly contribute to the hAGRP(87−132) binding. The mMC4R Phe259Ser and Phe254Ser residue mutations have been previously reported to result in agonist activity of the melanocortin-based antagonists SHU9119 and SHU9005 that appears to be specific for the melanocortin-based peptide antagonists, not for hAGRP.[20,31]

Additional putative interactions of the hAGRP(87−132) ligand amino acids with the mMC4R receptor residues have been identified outside the conserved hAGRP(111−113) Arg-Phe-Phe region (Figure 1 and Table 1). The hAGRP Arg89 and Ser93 amino acid side chains appear to interact with the mMC4R Cys271 (EL3, juxtapose to the extracellular start of TM7) backbone amide bond. The hAGRP His91 amino acid side chain is observed to interact with the mMC4R Asp103 (EL1) backbone carbonyl, Thr104 (EL1) side chain, and the Tyr33 (interface of the N-terminus and TM1) side chain hydroxyl moiety. The hAGRP Glu92 side chain is observed to form intramolecular contacts with the hAGRP Arg89 side chain consisting of putative electrostatic interactions. hAGRP Gln97 was observed to possess potential molecular interactions with the mMC4R Asp181 and intramolecularly with the hAGRP Asn114 amino acid. The hAGRP Gln98 putatively interacts with the mMC4R Asn266 amino acid residue located in EL3. Interestingly, a polymorphism of the human MC4R in morbidly obese humans has been identified, changing the homologous Asn274 (Asn266 mouse numbering) amino acid to a Ser residue.[32] The hAGRP Tyr109 side chain appears to form electrostatic interactions with the mMC4R Asp114 (TM3) residue. The hAGRP Asn114 side chain has been identified to form electrostatic interactions with the mMC4R Asp181 (interface between EL2 and TM4) amino acid side chain and hAGRP Gln97 amino acid. The hAGRP Phe116 benzyl side chain is observed to possess intramolecular side chain interactions with the hAGRP Tyr118 side chain juxtapose to the "core" hAGRP(109−118) decapeptide sequence. In addition to the hAGRP Tyr118 amino acid interacting intramolecularly with the hAGRP Phe116 side chain, the Tyr118 hydroxy moiety also appears to form electrostatic interactions with the mMC4R Asp105 and Gln107 (EL1) side chains. Interestingly, the hAGRP Arg120 amino acid side chain appears to form electrostatic interactions with the mMC4R Asp105 and Asp114 (TM3) residues, the latter identified by experimental data to be important for putative melanocortin ligand−receptor interactions.[20,26,28,33−35] The hAGRP Lys121 side chain putatively interacts with the mMC4R Asp103 (EL1) and hAGRP Asp103 residues, while the hAGRP Thr124 side chain may possess weak interactions with the mMC4R Thr110 (TM3) side chain. The hAGRP Arg131 amino acid appears to interact with the backbone of the mMC4R Ala106 residue. Finally, the C-terminal hAGRP Thr132 residue side chain may interact with the mMC4R Thr104 (EL1) residue side chain. The significance of

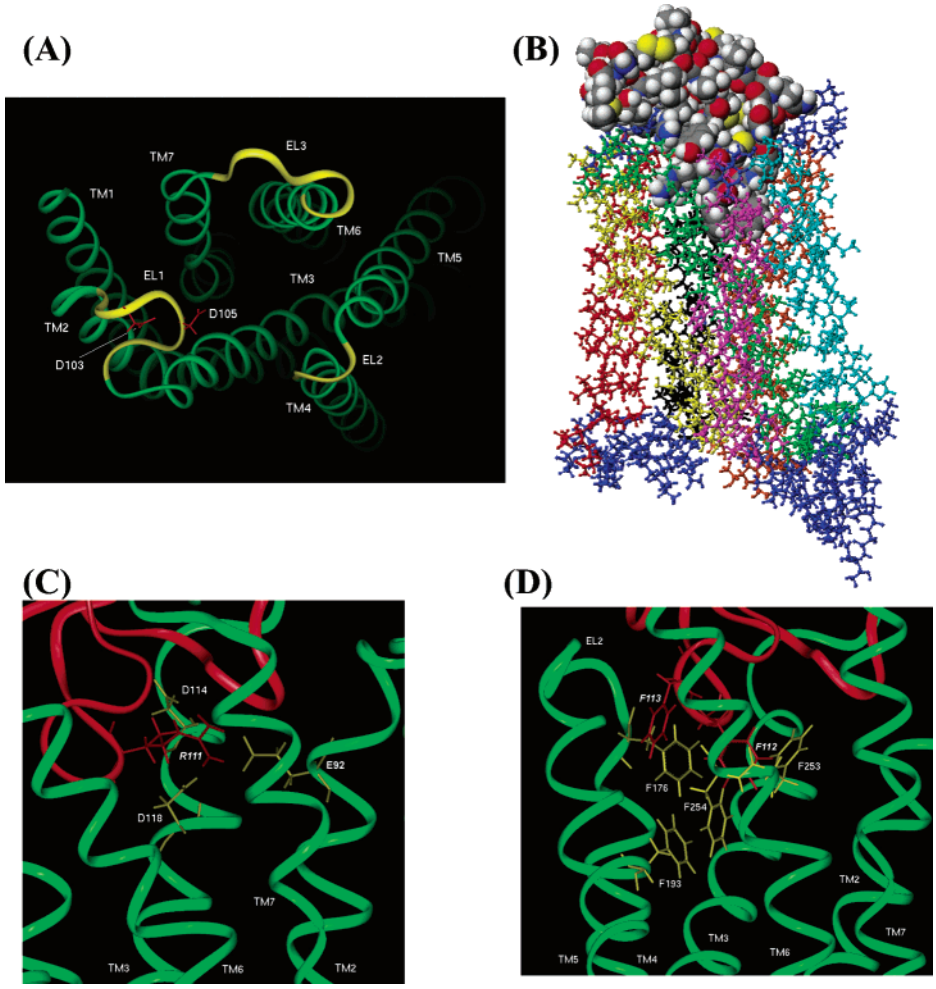

Figure 2. Model of the hAGRP(87−132)−mMC4R complex. (A) mMC4R receptor model (TM helical bundle and extracellular domain) viewed along the helical axes from the extracellular end. The TM helices are colored green, and extracellular loops are colored yellow. Side chains of Asp103 and Asp105 acidic residues in EL1 are highlighted. (B) Structural model of the hAGRP-(87−132)−mMC4R structure, visualized using CAChe V5.0, showing that the protein interacts with both the extracellular loops and an intramembrane binding site. AGRP is colored by atom type: C, black; O, red; N, blue; H, white; S, yellow. TM helical domains are the following: 1, red; 2, yellow; 3, green; 4, purple; 5, cyan; 6, orange; 7, black. Loops are colored blue. (C) Illustration of the hydrophilic binding pocket for AGRP(87−132) in mMC4R. The receptor and ligand are depicted as ribbons in green and red, respectively. The side chains of the important residues involved in the ionic bridge are highlighted and labeled. (D) Illustration of the hydrophobic binding pocket for AGRP(87−132) in mMC4R. The receptor and ligand are depicted as ribbons in green and red, respectively. The side chains of the important residues involved in the aromatic interaction are highlighted and labeled.

Table 2. Secondary Structure Prediction and Sequence Homology Analyses of the Extracellular and Intracellular Loop Region of the Mouse Melanocortin-4 Receptor

mMC4R loop	protein template[a]	residue range	sequence[b] and prediction[c]		fit rms[d]	homology (%)
EL1	mMC4R	101−108	**STDTDAQS**	*CCCCCEEC*		
	1ALO	323−330	**EIHPGTPN**	*CCCCCEEC*	0.5847	69.23
EL2	mMC4R	178−180	**IYS**	*CEE*		
	2HPD	196−198	**PAY**	*CEE*	0.3348	16.67
EL3	mMC4R	264−271	**PQNPYCVC**	*CCCCEEEC*		
	1RHD	171−178	**LESKRFQL**	*CCCCEEEC*	0.2784	29.81
IL1	mMC4R	65−68	**NKNLH**	*CEEEC*		
	1ACC	190−193	**EGYTV**	*CCEEC*	0.4479	34.88
IL2	mMC4R	145−153	**YALQYHNIM**	*CCCCCCCEE*		
	1TOF	53−61	**YAGKVIFLK**	*CCCEEEEEC*	0.2255	49.47
IL3	mMC4R	208−229	**FLMARLHIKR**	**IAVLPGTGTI RQ**		
			CCCCCCCEEE	*EEECCCCCEE EC*		
	1DOI	93−114	**VEDKNVRLTC**	**IGSPDADEVK IV**		
			CCCCCEEEEE	*ECCCCCCEEE EC*	0.5186	46.93

[a] Protein templates are identified by their PDB entry names. [b] Sequences are shown using the amino acid one-letter code. [c] Secondary structure prediction obtained using the method of GOR 4.0. α helix = *H*. *β* sheet = *E*. Random coil = *C*. [d] rms deviations of the anchor region between receptor loop and template.

these putative hAGRP(87−132) amino acid interactions with various mMC4R residues remains to be experimentally determined; however, insight into possible hAGRP(87−132)−mMC4R potentiating molecular interactions has been identified that may explain differences in AGRP ligand and receptor based pharmacology.

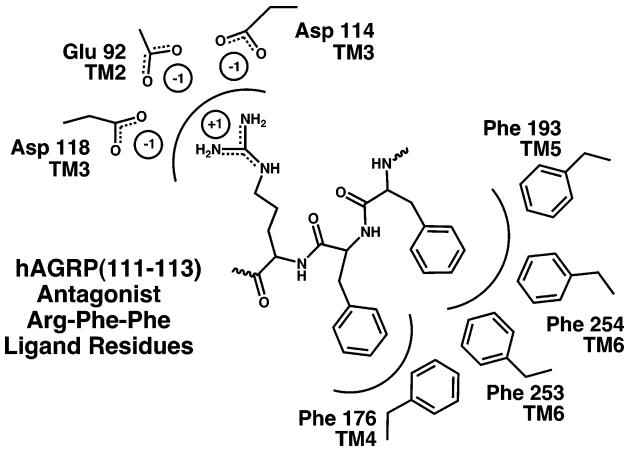

Figure 3. Illustration of the putative antagonist hAGRP-(111−113) Arg-Phe-Phe amino acid interactions with the mMC4R residues located in the transmembrane "binding" domain.

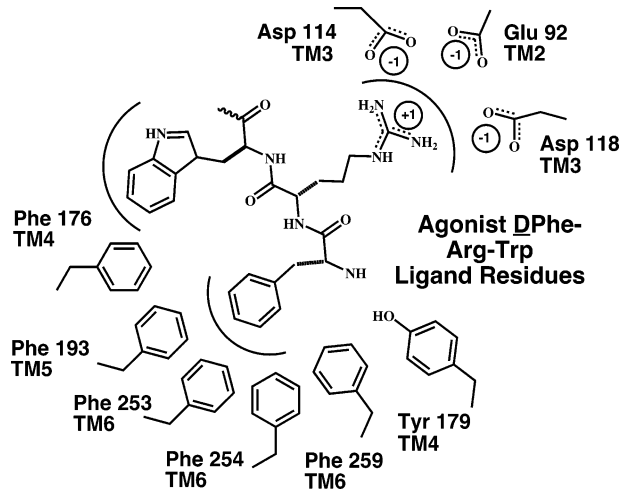

Figure 4. Illustration of the putative melanocortin agonist DPhe-Arg-Trp amino acid interactions with the mMC4R residues located in the transmembrane "binding" domain previously reported.

Initial attempts, presented herein, to validate the putative hAGRP−mMC4R interactions identified from this modeling study are presented below in the context of ligand design using a combination of the hAGRP antagonist peptide and melanocortin agonist His/Phe-Arg-Trp residues to generate chimeric peptides.

Biological Evaluation of Chimeric Peptides. The peptides reported herein were synthesized using standard fluorenylmethyloxycarbonyl (Fmoc)[36,37] or *tert*-butyloxycarbonyl (Boc)[38] chemistries. The peptides were purified to homogeneity using semipreparative reversed-phase high-pressure liquid chromatography (RP-HPLC). The peptides possessed the correct molecular weights, as determined by mass spectrometry. The purity of these peptides were assessed by analytical RP-HPLC in two diverse solvent systems. Table 3 summarizes the pharmacological results of control peptides and the chimeric AGRP−melanocortin peptides prepared in this study at the mouse melanocortin receptor MC1R, MC3−5R isoforms.

hAGRP(109−118) Based Template. Table 3 summarizes the pharmacological results of the peptides based on the AGRP(109−118) and "mini"-AGRP templates at the melanocortin receptors. The disulfide bridge containing AGRP(109−118) peptide has been previously identified as a submicromolar MC4R antagonist and micromolar MC1R agonist,[39,40] consistent with the results presented herein. For peptides **1**−**9**, a lactam bridge replaced the disulfide bridge of the AGRP(109−118) ligand to facilitate on-resin cyclization using Boc chemistry. The use of the Dpr amino acid to form the lactam bridge results in the same size membered ring as the disulfide bridge. To verify that the hAGRP(111−113) Arg-Phe-Phe amino acids are critical to melanocortin receptor molecular recognition and stimulation, peptide **1** was synthesized as a control, replacing these Arg-Phe-Phe residues with Ala's, and resulted in a lack of agonist or antagonist activity at the melanocortin receptors at up to 100 μM concentrations and was unable to competitively displace radiolabeled [^{125}I]-NDP-MSH beyond a ligand 25% binding at 10 μM concentrations. Peptide **2**, containing the lactam bridge instead of the disulfide bridge, resulted in equipotent MC1R agonist activity (within the inherent 3-fold experimental error), possessed micromolar MC3R antagonism, and was 8-fold less potent at the MC4R than hAGRP(109−118). Since the precise orientation and correlation between the antagonist AGRP Arg-Phe-Phe (111−113) amino acids and the melanocortin based Phe-Arg-Trp (7−9) was unknown, both the Phe-Arg-Trp and Trp-Arg-Phe orientations were introduced into the AGRP based template. Peptide **3** (Trp-Arg-Phe orientation) resulted in a micromolar MC1R agonist and a partial agonist at the MC4R but lacked any MC4R antagonism. Interestingly, when the Trp-Arg-D-Phe amino acids were substituted at the hAGRP 111−113 positions (peptide **4**), full MC4R agonism resulted, in addition to becoming a full MC5R agonist, and had slightly stimulated the MC3R 100 μM concentrations. Peptide **5**, containing the Phe-Arg-Trp hAGRP(111−113) orientation, resulted in a full micromolar agonist at the MC1, MC4, and MC5 receptors. Incorporation of the D-Phe-Arg-Trp residues at the AGRP Arg-Phe-Phe (111−113) positions, peptide **6**, resulted in high nanomolar MC4R and MC5R agonists with equipotent MC1R micromolar agonist activity compared with that of the hAGRP(109−118) peptide. Peptide **7** consisted of adding the His amino acid of the melanocortin agonist putative message sequence, "His-Phe-Arg-Trp," into the lactam-modified hAGRP(109−118) template and resulted in a lack of MC4R agonist or antagonist activity but retained micromolar MC1R agonist activity equipotent with that of the hAGRP-(109−118) lead peptide. In peptide **8**, the His-Arg-Phe-Phe motif of peptide **7** was replaced with the His-Phe-Arg-Trp motif and resulted in nanomolar agonist activity at all the melanocortin receptor isoforms examined in this study. Finally, peptide **9** consisting of the Tyr-c[Asp-His-D-Phe-Arg-Trp-Asn-Ala-Phe-Dpr]-NH_2 sequence resulted in subnanomolar full agonist activity at the MC1 and MC3−5 receptors, was equipotent to α-MSH at the MC1R, MC3R, and MC5R, but was ca. 30-fold more potent than α-MSH at the MC4R.

Mini-AGRP Based Template. The design, synthesis, pharmacology at the human melanocortin receptors, and three-dimensional NMR structure of "mini"-AGRP has been described previously by Jackson et al.[29] The pharmacology at the mouse melanocortin receptors, primary sequence, and disulfide bridges of Ac-mini-

Table 3. Pharmacology of the Chimeric Melanocortin−hAGRP Peptides Using the hAGRP(109−118) Template with the hAGRP(111−113) Arg-Phe-Phe Amino Acids Replaced by Melanocortin Agonist His-Phe-Arg-Trp Residues at the Various Indicated Positions (Bold)[a]

		mMC1R		mMC3R		mMC4R		mMC5R	
Peptide	**Structure**	EC_{50} (nM)	Fold Difference	EC_{50} (nM)	Fold Difference	EC_{50} (nM)	Fold Difference	EC_{50} (nM)	Fold Difference
α-MSH	Ac-Ser-Tyr-Ser-Met-Glu-His-Phe-Arg-Trp-Gly-Lys-Pro-Val-NH_2	0.55±0.09		0.79±0.14		5.37±0.62		0.44±0.09	
NDP-MSH	Ac-Ser-Tyr-Ser-**Nle**-Glu-His-**DPhe**-Arg-Trp-Gly-Lys-Pro-Val-NH_2	0.038±0.012		0.098±0.013		0.21±0.03		0.071±0.012	
MTII	Ac-Nle-c[Asp-His-DPhe-Arg-Trp-Lys]-NH_2	0.020±0.003		0.16±0.03		0.087±0.008		0.16±0.03	
hAGRP(87-132)		>100,000		pA_2=8.9±0.2		pA_2=9.4±1.0		>100,000	
hAGRP(109-118)	Tyr-c[Cys-**Arg-Phe-Phe**-Asn-Ala-Phe-Cys]-Tyr-NH_2	5,120±3,040	1	>100,000		pA_2=6.8±0.24	1	>100,000	1
1	Tyr-c[Asp-**Ala-Ala-Ala**-Asn-Ala-Phe-Dpr]-Tyr-NH_2	>100,000		>100,000		>100,000		>100,000	
2	Tyr-c[Asp-**Arg-Phe-Phe**-Asn-Ala-Phe-Dpr]-Tyr-NH_2	1,730±310	**3**	pA_2=5.7±0.2	**1**	pA_2=5.9±0.2	**8**	>100,000	
3	Tyr-c[Asp-**Trp-Arg-Phe**-Asn-Ala-Phe-Dpr]-Tyr-NH_2	13,500±3,100	**3**	>100,000		Partial agonist 15,900±7,300		>100,000	
4	Tyr-c[Asp-**Trp-Arg-DPhe**-Asn-Ala-Phe-Dpr]-Tyr-NH_2	6,120±2,300	**1**	SA 45% at 100μM		10,900±2,900		2,220±1,100	**>-45**
5	Tyr-c[Asp-**Phe-Arg-Trp**-Asn-Ala-Phe-Dpr]-Tyr-NH_2	19,700±4,300	**4**	SA 38% at 100μM		13,400±400		3,900±1,800	**>-25**
6	Tyr-c[Asp-**DPhe-Arg-Trp**-Asn-Ala-Phe-Dpr]-Tyr-NH_2	4,850±1,450	**1**	SA 46% at 100μM		450±160		124±25	**>-800**
7	Tyr-c[Asp-**His-Arg-Phe-Phe**-Asn-Ala-Phe-Dpr]-Tyr-NH_2	13,300±1,700	**3**	SA 40% at 100μM		>100,000		>100,000	
8	Tyr-c[Asp-**His-Phe-Arg-Trp**-Asn-Ala-Phe-Dpr]-Tyr-NH_2	59.5±16.7	**-86**	309±120	**>-320**	57.1±4.4		90.0±22.0	**>-1,100**
9	Tyr-c[Asp-**His-DPhe-Arg-Trp**-Asn-Ala-Phe-Dpr]-Tyr-NH_2	0.21±0.09	**-24,000**	0.99±0.34	**>-100,000**	0.18±0.04		0.55±0.14	**>-180,000**
Ac-Mini-hAGRP-NH_2	Ac-hAGRP(87-120, Cys105Ala)-NH_2	>100,000		pA_2=8.08±0.1		pA_2=8.46±0.06		>100,000	
Ac-Mini-(His-DPhe-Arg-Trp)hAGRP-NH_2		0.16±0.02		29.8±5.5		1.40±0.29		0.56±0.28	

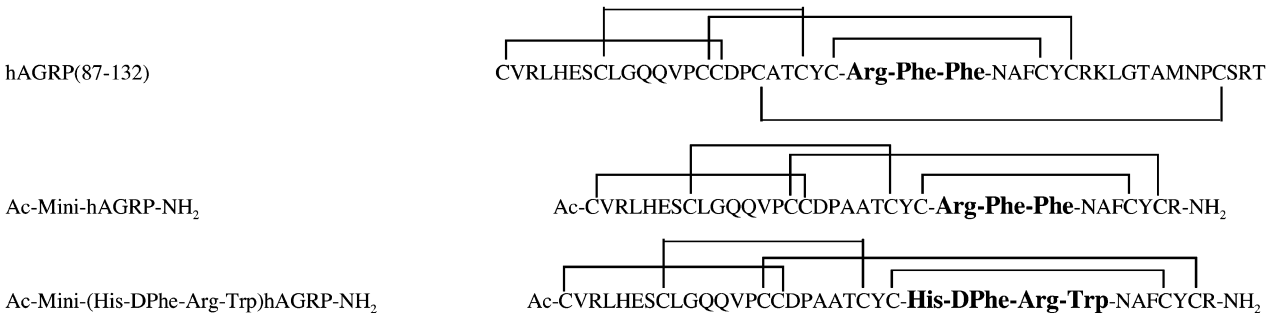

[a] The indicated errors represent the standard error of the mean determined from at least three independent experiments. The antagonistic pA_2 values were determined using the Schild analysis and the agonist MTII. >100000 indicates that the compound was examined but lacked agonist or antagonist properties at up to 100 μM concentrations. SA denotes the percent maximal stimulatory response observed at 100 μM concentrations but not enough stimulation was observed determine an EC_{50} value.

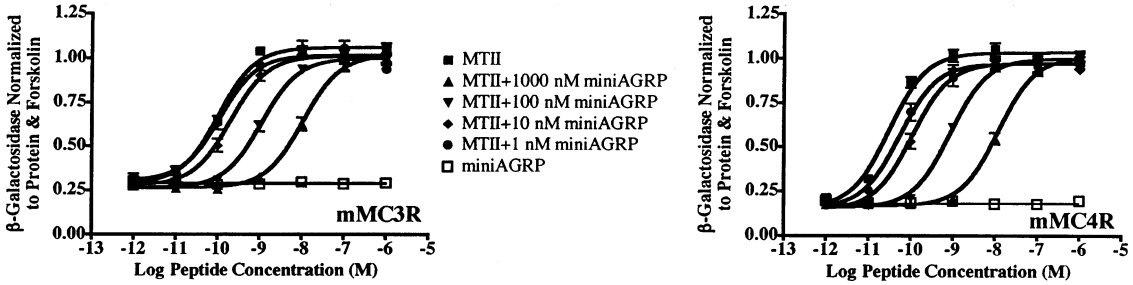

Figure 5. Competitive antagonist pharmacology of Ac-mini-hAGRP-NH_2 at the mouse melanocortin-3 and -4 receptors.

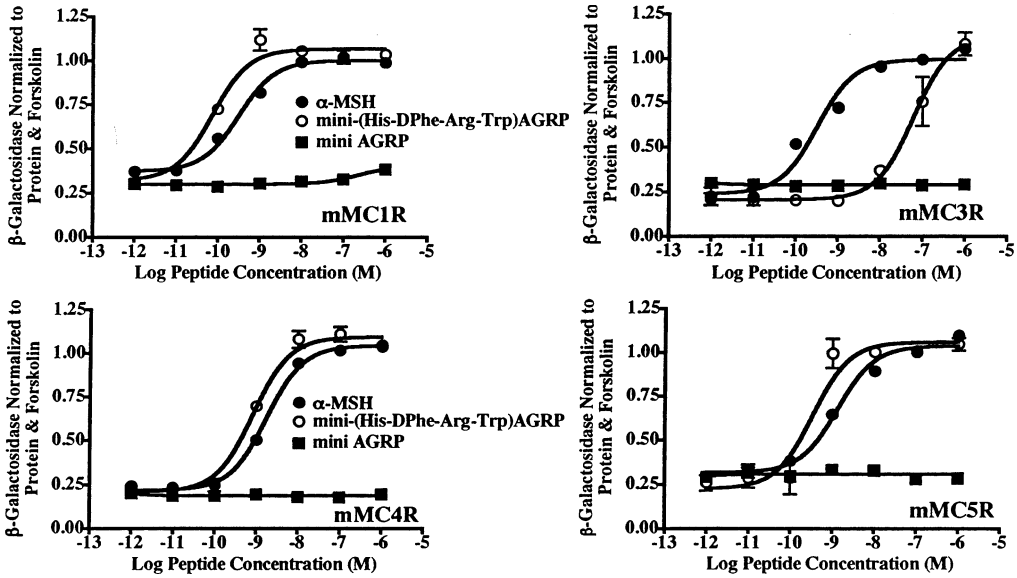

Figure 6. Illustration of the mouse melanocortin receptor agonist pharmacology comparing the α-MSH (endogenous melanocortin receptor agonist), Ac-mini-AGRP-NH_2 (no agonist activity), and Ac-mini-(His-D-Phe-Arg-Trp)hAGRP-NH_2 (full agonist).

Table 4. Competitive Displacement Binding Results of the Chimeric Melanocortin−hAGRP Peptides Using the hAGRP(109−118) Template with the hAGRP(111−113) Arg-Phe-Phe Amino Acids Replaced by Melanocortin Agonist His-Phe-Arg-Trp Residues at the Various Indicated Positions (Bold) at the Mouse Melanocortin-4 Receptor Using Radiolabeled NDP-MSH and hAGRP(87−132)[a]

peptide	structure	[^{125}I]-NDP-MSH IC_{50} (nM)	[^{125}I]-hAGRP(87−132) IC_{50} (nM)
NDP-MSH*	Ac-Ser-Tyr-Ser-**Nle**-Glu-His-**DPhe**-Arg-Trp-Gly-Lys-Pro-Val-NH_2	4.22 ± 0.48	ND
hAGRP(87−132)*		ND	5.48 ± 0.78
2	Tyr-c[Asp-**Arg-Phe-Phe**-Asn-Ala-Phe-Dpr]-Tyr-NH_2	4800 ± 380	3200 ± 690
3	Tyr-c[Asp-**Trp-Arg-Phe**-Asn-Ala-Phe-Dpr]-Tyr-NH_2	10300 ± 4000	7300 ± 1000
4	Tyr-c[Asp-**Trp-Arg-DPhe**-Asn-Ala-Phe-Dpr]-Tyr-NH_2	>10 μM	>10 μM
5	Tyr-c[Asp-**Phe-Arg-Trp**-Asn-Ala-Phe-Dpr]-Tyr-NH_2	9200 ± 240	4100 ± 1200
6	Tyr-c[Asp-**DPhe-Arg-Trp**-Asn-Ala-Phe-Dpr]-Tyr-NH_2	6800 ± 470	3100 ± 2300
8	Tyr-c[Asp-**His-Phe-Arg-Trp**-Asn-Ala-Phe-Dpr]-Tyr-NH_2	540 ± 170	290 ± 220
9	Tyr-c[Asp-**His-DPhe-Arg-Trp**-Asn-Ala-Phe-Dpr]-Tyr-NH_2	0.96 ± 0.13	0.26 ± 0.05
Ac-Mini-hAGRP-NH_2	Ac-hAGRP(87−120, Cys105Ala)-NH_2	29.8 ± 28	4.74 ± 4.6
Ac-Mini-(His-DPhe-Arg-Trp)hAGRP-NH_2		1.46 ± 0.88	4.45 ± 4.8

[a] The asterisk (*) indicates results obtained from greater than 11 independent experiments. ND indicates not determined in this study. Compounds that did not possess any functional pharmacology were excluded from these studies. The indicated errors represent the standard deviation of the mean determined from at least two independent experiments. >10 μm indicates that the compound was examined but lacked the ability to competitively displace the radiolabeled compound to 50% maximum response (IC_{50}) at up to 10 μM concentrations.

AGRP(87−120, C105A)-NH_2 are presented in Table 3. The pharmacology observed for Ac-mini-AGRP(87−120, C105A)-NH_2 at the mouse melanocortin receptors, reported herein (Table 3, Figures 5 and 6), is consistent, within experimental error, with those reported previously at the corresponding human melanocortin receptors.[29] After we observed that substitution of the hAGRP Arg-Phe-Phe (111−113) residues by the agonist His-D-Phe-Arg-Trp sequence in peptide **9** resulted in potent melanocortin receptor agonists, a similar substitution was made in the mini-AGRP sequence. Notably, the Ac-mini-(His-D-Phe-Arg-Trp)AGRP-NH_2 peptide resulted in a potent nanomolar full agonist at the mMC1 and MC3−5 receptors (Table 3 and Figure 6). Thus, substitution of the hAGRP Arg-Phe-Phe residues by the agonist His-D-Phe-Arg-Trp sequence converted a potent MC3R and MC4R antagonist into a potent agonist at all the melanocortin receptors studied herein.

Competitive Displacement Binding Studies at the Mouse MC4R. Since we are hypothesizing that a common binding pocket is present in the mouse MC4R where both the endogenous agonists and antagonists interact, and specifically that the hAGRP Arg-Phe-Phe-(111−113) antagonist residues putatively interact with

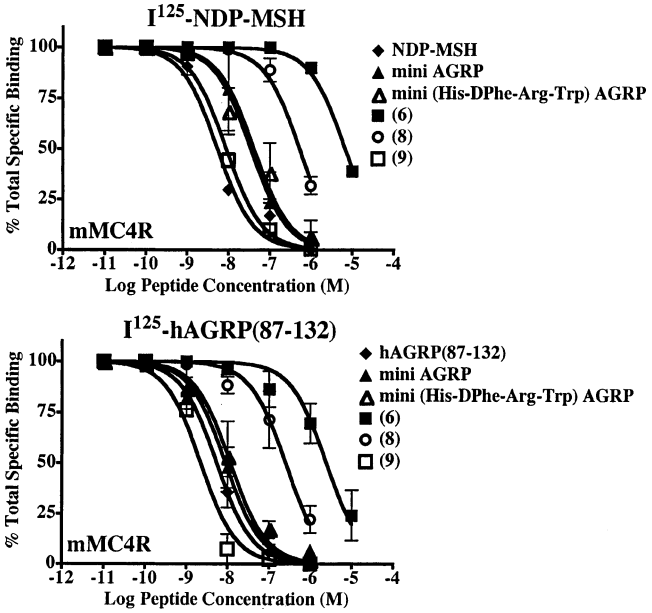

Figure 7. Competitive displacement binding studies at the mouse melanocortin-4 receptor of select compounds. Both [^{125}I]-NDP-MSH and [^{125}I]-hAGRP(87−132) were used to competitively displace the indicated ligands.

the mMC4R in a similar manner as the agonist Phe-Arg-Trp(7−9, α-MSH numbering), we have performed competitive displacement binding assays using both radiolabeled [^{125}I]-NDP-MSH and [^{125}I]-hAGRP(87−132).[20] Table 4 summarizes the ligand binding inhibitory concentrations at 50% maximal response (IC_{50}) values obtained. Figure 7 illustrates the ability of selected compounds to competitively displace radiolabeled [^{125}I]-NDP-MSH or [^{125}I]-hAGRP(87−132) with similar binding affinities. These data illustrate that the binding pharmacology is consistent with the functional β-galactosidase cAMP based reporter gene assay, as previously reported,[41] at the mMC4R, within only up to 5- to 15-fold differences in a direct comparison of EC_{50} to IC_{50} values.

Discussion

Since the discovery of the only two known endogenous G-protein-coupled receptor antagonists, agouti[11,19] and agouti-related protein,[1,42,43] the characterization of the melanocortin-4 receptor as being involved in food intake, obesity, and energy homeostasis,[2,44] and the MC4R as a receptor for both agouti and AGRP, has resulted in the targeting of AGRP and the MC4R for drug discovery efforts. In attempts to identify if the AGRP protein competitively antagonized the MC4 receptor by an overlapping putative binding site with the endogenous agonist α-MSH ligand, or if an allosteric mechanism of antagonism is the molecular mechanism(s) of blocking agonist stimulation at the MC4R, several MC4 receptor mutagenesis studies have been performed.[20,23,24,28] Additionally, ligands have been designed, synthesized. and pharmacologically characterized on the basis of the AGRP antagonist template, in attempts to identify hAGRP amino acids important for MC4R molecular recognition and antagonism.[29,35,39,45−53] To date, these studies have identified that (1) AGRP has both unique and identical putative MC4R binding and molecular recognition interactions as the melanocortin agonists,[20,24,28] (2) both radiolabeled antagonist [^{125}I]-AGRP-(87−132) and agonist [^{125}I]-NDP-MSH can competitively displace AGRP(87−132), mini-AGRP, and truncated monocyclic analogous of hAGRP[29,35,54] with similar affinities, and (3) AGRP is a competitive antagonist of melanocortin agonists (not an allosteric antagonist or modulator),[1,20,28,54] presenting strong experimental evidence that there are putative hAGRP residue interactions with the MC4R that are common with the melanocortin agonists.

Putative hAGRP(87−132)−Mouse Melanocortin-4 Receptor Interactions. In rationale attempts to identify specific putative antagonist hAGRP(87−132) ligand amino acid interactions with the mouse MC4 receptor residues, in addition to those postulated on the basis of receptor mutagenesis studies, three-dimensional homology molecular modeling was performed using the high-resolution NMR based structure of hAGRP(87−132)[22] and the GPCR rhodopsin[21] templates. Both putative intramolecular hAGRP(87−132) amino acid interactions and hAGRP(87−132)−mMC4R intermolecular contacts were identified and are summarized in Table 2. Figure 4 summarizes the putative melanocortin agonist D-Phe-Arg-Trp interactions with the mMC4R reported previously,[20] while Figure 3 summarizes the putative antagonist hAGRP(111−113) Arg-Phe-Phe interactions with the mMC4R resulting from the study presented herein. Interestingly, both the antagonist hAGRP Arg111 and agonist Arg^8 (α-MSH numbering) putatively interact with the same mMC4R residues Glu92 (TM2), Asp114 (TM3), and Asp 118 (TM3) that have been previously demonstrated by MC4R in vitro mutagenesis studies to be important for hAGRP(87−132) and melanocortin agonist ligand binding and functional activity.[20,28] Comparison of the putative antagonist hAGRP Phe112 and Phe113 residue interactions with the mMC4R versus the putative melanocortin agonist D-Phe^7 and Trp^9 (α-MSH numbering) amino acid interactions with the mMC4R residues (Figures 3 and 4) reveals interesting observations. First, four mMC4R receptor−ligand interactions appear to be consistent for binding to both the antagonist hAGRP Phe112-Phe113 amino acids and the agonist D-Phe-Trp amino acids, specifically the mMC4R Phe176 (TM4), Phe193 (TM5), Phe253 (TM6), and Phe254 (TM6) residues. Previous mMC4R in vitro mutagenesis studies identified when these three Phe176 (TM4), Phe253 (TM6), and Phe 254 (TM6) mMC4R Phe residues were mutated to Phe176Lys, Phe253Ser, and Phe254Ser, dramatic changes in melanocortin-based agonist/antagonist and hAGRP(83−132) binding and/or functional activity resulted,[20] supporting the hypothesis of common putative antagonist hAGRP Phe112-Phe113 and melanocortin agonist Phe^7-Trp^9 interactions with the mMC4R. Second, the mMC4R aromatic network putatively interacting with the melanocortin agonist D-Phe-Trp amino acids is more extensive than the mMC4R Phe residues interacting with the hAGRP Phe112-Phe113 amino acids. These observations are consistent with the general theory for GPCR receptor stimulation suggesting that an agonist potentially interacts with several receptor residues and is a more "complex" interaction/mechanism with the receptor than would be observed for putative competitive antagonist−receptor interactions that simply block the

agonist from stimulating the receptor and "locking" the receptor into an "off" position.

A contemporary concept regarding the molecular interactions of large peptide ligands, like AGRP, and GPCRs suggests that hAGRP(87−132) amino acids may interact with both the receptor transmembrane domain and the receptor exoloops.[23,24] The AGRP−MC4R complex model generated in this study illustrates putative exoloops and TM ligand−MC4 receptor interactions, summarized in Table 1 and Figure 1. Specifically, Gln97 and Gln98 of hAGRP (87−132) putatively form electrostatic side chain to side chain interactions with the mMC4R exoloop amino acid Asn266 (EL3) and Asp181 (EL2 juxtapose the initiation of TM5) residues. These putative AGRP Gln−melanocortin exoloop interactions are consistent with the cassette substitution experimental results reported by Yang et al.[23,24] that suggested the important role of EL2 and EL3 of the hMC4R in hAGRP(87−132) but not the truncated hAGRP(110−117) monocyclic derivative binding. However, on the basis of these hMC4R cassette mutagenesis studies, inconsistency exists for EL1's role in interacting with the AGRP(87−132) ligand.[23,24] In the AGRP(87−132)−mMC4R model complex presented herein, it was observed that the conserved melanocortin receptor acidic motif consisting of the mMC4R(103−105) Asp-X-Asp located in EL1 putatively interacts with hAGRP(87−132) amino acids. The mMC4R Asp105 potentially forms hydrogen bonds with Tyr118 and Arg120 of AGRP(87−132), while the mMC4R Asp103 is putatively hydrogen-bonded to Lys121 of hAGRP(87−132). However, the MC4R exoloop swapping experiment concluded a lack of the EL1 contributing to hAGRP(87−132) ligand−MC4R interactions.[23,24] A comparison of the chimeric receptor model used to perform these exoloops swapping experiments[23,24] with our current model derived from the more recent rhodopsin crystal structure[21] indicates that the definitions of the exoloop boundaries were modified from the previous rhodopsin and bacteriarhodopsin structures[55] proposed for the melanocortin receptors and used in the design of the chimeric receptors.[25] Thus, the precise involvement of the proposed specific interactions of the MC4R exoloop regions with the hAGRP(87−132) antagonist needs to be further examined by experimental methods from both the receptor and ligand perspective. The three-dimensional homology molecular model of the antagonist hAGRP-(87−132)−mMC4 receptor complex proposed herein potentially provides insight into putative "key" ligand−receptor interactions important for molecular recognition, binding, functional activity, and potentiating hAGRP residue−receptor interactions that can be critically examined and experimentally tested for validity.

AGRP-Melanocortin Peptide Chimeric Ligands at the Mouse Melanocortin-4 Receptor. In attempts to validate the homology molecular model of the hAGRP-(87−132)−mMC4 receptor complex presented herein, chimeric ligands consisting of a hAGRP monocyclic template substituted with melanocortin agonist "core" residues were designed, synthesized, and pharmacologically characterized at the mouse melanocortin-4 receptor (Table 3). Additionally, these ligands were generated to more directly test the hypothesis that the hAGRP(111−113) Arg-Phe-Phe amino acids may putatively interact

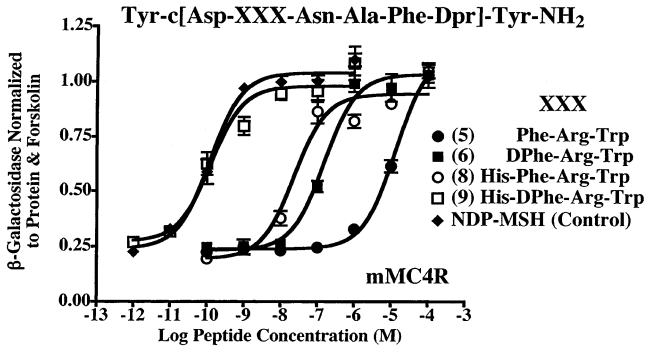

Figure 8. Agonist pharmacology of the chimeric hAGRP−melanocortin peptides containing the His/Phe-Arg-Trp residues, indicated by XXX, at the mouse melanocortin-4 receptor.

with the mMC4R residues in a similar manner as the melanocortin agonist DPhe-Arg-Trp amino acids. When the antagonist hAGRP key Arg-Phe-Phe (111−113) residues are substituted with the melanocortin agonist Phe-Arg-Trp amino acids (peptide **5**) a weak micromolar agonist resulted at the mMC4R (Figure 8). Epimerization from the natural L-configuration to the D-configuration at the Phe 7-position of melanocortin agonist peptides characteristically results in enhanced melanocortin-based agonist or antagonist potency.[31,56−59] This melanocortin agonist attribute of enhancing ligand potency by stereochemical inversion of the Phe residue was tested in the chimeric AGRP template (peptide **6**, Figure 8), and consistent with the known structure−activity relationships (SAR) of melanocortin agonists, a 29-fold increase in potency was observed at the mMC4R (comparing peptides **5** and **6**, Figure 8). An additional structural trait of melanocortin agonist based SAR is that the presence of the His at the N-terminal of the Phe-Arg-Trp sequence results in enhanced potency.[28,59,60] Consistent with these data, comparisons of peptides **5** and **6** with peptides **8** and **9**, respectively, resulted in 230- and 2500-fold increased mMC4R agonist ligand potency (Figure 8). In an independent study, the hAGRP(111−113) Arg-Phe-Phe amino acids were substituted for the melanocortin agonist D-Phe-Arg-Trp amino acids in both the linear NDP-MSH and cyclic MTII peptide templates.[53] These latter studies resulted in ligands that ranged significantly in pharmacology from full nanomolar agonists to ligands that lacked melanocortin receptor functional activity (mMC1R and mMC3−5R), depending upon the template, substitution, and stereochemistry.[53] Taken together, these data support the hypothesis that the hAGRP(111−113) Arg-Phe-Phe amino acids may putatively interact with the mMC4R residues in a similar manner as the melanocortin agonist D-Phe-Arg-Trp amino acids. To further investigate this hypothesis, and on the basis of the potent mMC4R pharmacology observed for peptide **9**, the antagonist hAGRP Arg-Phe-Phe (111−113) residues were replaced with the melanocortin agonist His-D-Phe-Arg-Trp residues in the mini-AGRP template (Table 3) and interestingly resulted in a potent nanomolar agonist at the mMC4R but also at the mMC1, mMC3, and mMC5 receptors (Figure 6). Thus, these data presented herein provide experimental evidence, from the ligand perspective, that the homology molecular model of the hAGRP(87−132)−mMC4R complex may be a valuable tool for the understanding of putative ligand−MC4

receptor interactions that can be further experimentally tested and utilized for the design of MC4R ligands for the treatment of obesity and type 2 diabetes related diseases.

Melanocortin Receptor Selectivity. The central MC3 and MC4 receptors expressed in the brain have been associated with the physiological role of weight and energy homeostasis through the use of knockout mice and in vivo feeding studies.[2,44,61,62] Because of the neuroanatomical overlap in some regions of the brain of the MC3 and MC4 receptor mRNA and the complexity of energy homeostatic pathways, melanocortin ligands selective for either of these melanocortin receptor isoforms are desirable for in vivo studies. In the study presented herein, peptide **6** (Tyr-c[Asp-DPhe-Arg-Trp-Asn-Ala-Phe-Dpr]-Tyr-NH_2) resulted in a ligand that is only a slight mMC3R agonist (is not an mMC3R antagonist and does not bind at the mMC3R with greater than 25% specific binding at 10 μM concentrations) but possesses a 450 nM agonist EC_{50} value at the mMC4R, resulting in a >200-fold MC4R versus MC3R selective compound. Interestingly, while hAGRP and Ac-mini-AGRP-NH_2 did not possess any significant receptor selectivity preferences for either the mMC3R or mMC4R (Table 3), the Ac-mini-(His-DPhe-Arg-Trp)hAGRP-NH_2 derivative possessed ca. 20-fold MC4R versus MC3R selectivity. These novel ligands, and their use as templates for melanocortin receptor selectivity, may prove to be interesting tools for further studies into "key" melanocortin ligand structural features important for central melanocortin receptor selectivity and potency.

Conclusions

The study presented herein describes the generation of a three-dimensional molecular model of the ligand−receptor complex of the antagonist hAGRP(87−132) and mMC4R. This is the first report of molecular modeling studies on the endogenous antagonist hAGRP(87−132) binding to melanocortin-4 receptor, based on the high-resolution rhodopsin crystal structure template. The model is consistent with the known AGRP ligand structure−activity studies and MC4R in vitro mutagenesis experimental data and validates the previously proposed "common" hydrophilic and aromatic binding pockets for melanocortin agonist and antagonist "key" ligand residues. This proposed hAGRP(87−132)−mMC4R homology molecular model complex has been initially experimentally tested herein by the design of chimeric hAGRP−melanocortin peptides resulting in agonist activity at the mMC4R. These studies provide additional experimental evidence supporting the hypothesis that the antagonist hAGRP(111−113) Arg-Phe-Phe residues may be mimicking the melanocortin agonist Phe-Arg-Trp amino acid interactions at the mMC4 receptor. Furthermore, notable results from the ligands presented herein include the identification of a novel potent subnanomolar melanocortin agonist template consisting of the sequence Tyr-c[Asp-His-DPhe-Arg-Trp-Asn-Ala-Phe-Dpr]-Tyr-NH_2 that can be utilized for future melanocortin receptor SAR studies. A new and novel peptide template has been identified that results in >200-fold selectivity for the MC4 versus the MC3 receptor (Tyr-c[Asp-DPhe-Arg-Trp-Asn-Ala-Phe-Dpr]-Tyr-NH_2). Finally, substitution of the antagonist hAGRP Arg-Phe-Phe(111−113) residues by the agonist His-D-Phe-Arg-Trp amino acids into the Ac-mini-AGRP-NH_2 template resulted in a potent melanocortin receptor agonist that possessed 20-fold MC4R versus MC3R selectivity.

Experimental Section

Three-Dimensional Homology Molecular Modeling of the Melanocortin-4 Receptor and Docking of hAGRP-(87−132) Computational Methods. The initial receptor model was derived from the C_α coordinate template of rhodopsin provided by Baldwin.[63] After the publication of the high-resolution 2.8 Å crystal structure of rhodopsin[21] (PDB code: 1F88), we rebuilt our receptor model based on this latter GPCR structure. The sequences of rhodopsin and melanocortin receptor were searched and retrieved from SRS 6.06 (European Bioinformatics Institute, EBI). All fragments and duplicates were discarded. The selected 42 rhodopsin sequences and 34 melanocortin receptor sequences plus the new mMC4R sequence were aligned using the program ClustalW 1.81[64] with the default parameters. The resulting multiple-sequence alignment was manually edited within the SeqLab of GCG Wisconsin Package to align the highly conserved GPCR residues.[65] Mutations and loop building were performed within the Biopolymer module implemented in SYBYL 6.5 (Tripos Inc.). Secondary structure predictions of the loop regions were carried out using GOR 4.0 method[66] as implemented in Biology Work Bench 3.2 (San Diego Supercomputer Center, SDSC). The N- (1−31) and C-terminals (311−on) of mMC4R were then deleted and capped with the acetylated N-terminus and *N*-methylamide C-terminus. Hydrogen atoms were added using the HBUILD module within CHARMM 25b2.[67,68]

The models were subjected to 1000 cycles of steepest descent followed by adopted basis Newton−Raphson algorithms until convergence of 0.01 kcal/(mol Å) rms deviation. A 1.0 kcal/mol positional constraint was applied to the receptor backbone atoms. The receptor was then placed in a restrained water droplet model[69] for further annealing refinement on the extracellular loop domain. The loops were fully solvated in a sphere of equilibrated TIP3P water[70] with a radius of 35 Å and free to move in the simulation. Restraints were applied to the transmembrane domain fixing all atoms except the side chains of the last one extracellular turn of the transmembrane helices. The starting structures for the simulated annealing studies were obtained from minimization, with additional positional restraints imposed on water oxygen atoms. The minimized structure was further refined using the following simulated annealing protocol: the system was gradually heated to 1500 K over a period of 30 ps with $\Delta T = 5$ K every 0.1 ps, followed by 10 ps of equilibration at 1500 K. Ten structures were extracted from the trajectory at 1500 K by sampling every 1 ps. Each structure was cooled to 300 K gradually with three additional 10 ps of constant temperature simulation at 700, 500, and 300 K. The restraints applied to the transmembrane domain were reduced gradually from 10 kcal/(mol Å^2) to 2 kcal/(mol Å^2) during the annealing process. The initial positional restraints of 0.1 kcal/(mol Å^2) imposed on water oxygen atoms were decreased gradually to zero from 1500 to 500 K, and then spherical harmonic restraints acted on the oxygen atoms of waters in the outer 5 Å shell of the solvation sphere instead. The force constant of the miscellaneous mean field potential (MMFP) potential was $K_R = 0.002$ kcal/(mol Å^2) from 500 to 400 K and $K_R = 0.0007$ kcal/(mol Å^2) from 400 to 300 K. The structures obtained at the end of 300 K were fully minimized and then analyzed on the basis of the energy criteria and the pairwise root-mean-square deviation analysis implemented in the Insight II 98.0 package (Biosym/MSI, San Diego). One of these structures was equilibrated at 300 K for 100 ps, and the receptor structure averaged over 62 ps to 80 ps was fully minimized until convergence.

The coordinates of AGRP(87−132) (Figure 2) were taken from the updated 2D ^{1}H NMR structure (PDB code: 1HYK).[22] The peptide was manually docked into the minimized mMC4

receptor structure via interactive graphics using the Docking module in Insight II. The key Arg-Phe-Phe amino acids of hAGRP(111−113)[39,40] were found to fit to the putative binding pocket of the mMC4R previously identified for the melanocortin agonists.[20,25] The resulting ligand−receptor complex was then "soaked" into the previous restrained water droplet model and applied the MMFP potential. The scope of restraints on the transmembrane domain was lowered to start from the third extracellular turn below the putative binding site. In vitro mutagenesis data of the mMC4R[20] were converted into distance constraints and employed in the subsequent minimization and dynamics. The whole system was energy-minimized and equilibrated for 50 ps with positional restraints applied on the transmembrane domain and ligand backbone atoms. During another 50 ps of running, the distance constraints were gradually reduced to zero and position restraints were reduced to 0.5 kcal/(mol Å^2) and zero on the transmembrane domain and ligand, respectively. Finally, the system was allowed to freely evolve during 200 ps of MD simulation at 300 K.

The molecular simulations were performed with the CHARMM 25b2 package using the param27 parameter set.[71−73] Molecular dynamics was carried out using the Verlet leapfrog algorithm with a distance-dependent dielectric constant $\epsilon = r$. Long-range electrostatic forces were cut off at 13 Å by means of a shifting function, and van der Waals forces were cut off between 9 and 13 Å by means of a switching function. The nonbonded list was kept to 14 Å and updated every 10 steps. A step size of 1 fs was used, and the velocities were scaled every 50 steps to keep the temperature within 10 of 300 K during the equilibration. All bonds containing hydrogens were held rigid by the SHAKE algorithm.[74] The calculations were performed on a Silicon Graphics Onyx2 supercomputer at the University of Florida McKnight Brain Institute.

Synthesis of Cyclic Lactam Bridge Containing Peptides. The chimeric hAGRP−melanocortin peptides were synthesized using standard Boc methodology[38,75] on an automated synthesizer (Advanced ChemTech 440MOS, Louisville, KY). The amino acids Boc-Tyr(2ClBzl), Boc-diaminopropionic acid [Dpr(Fmoc)], Boc-Asp(OFm), Boc-Arg(Tos), Boc-Phe, Boc-His(Bom), Boc-D-Phe, Boc-Trp(CHO), Boc-Asn, and Boc-Ala were purchased from Bachem (CA). The coupling reagents benzotriazol-1-yl-oxytris(dimethyloamino)phosphonium hexafluorophosphate (BOP), *O*-benzotriazolyl-*N*,*N*,*N*′,*N*′-tetramethyluronium hexafluorophosphate (HBTU), and 1-hydroxybenzotriazole (HOBt) were obtained from Peptides International. Glacial acetic acid (HOAc), dichloromethane (DCM), methanol (MeOH), acetonitrile (ACN), and anhydrous ethyl ether were purchased from Fisher (Fair Lawn, NJ). *N*,*N*-Dimethylformamide (DMF) was purchased from Burdick and Jackson (McGaw Park, IL). Trifluoroacetic acid (TFA), 1,3-diisopropylcarbodiimide (DIC), pyridine, dimethyl sulfoxide (DMSO), piperidine, phenol, and acetic anhydride were purchased from Sigma (St. Louis, MO). *N*,*N*-Diisopropylethylamine (DIEA), 1,2-ethanedithiol (EDT), and triisopropylsilane (TIS) were purchased from Aldrich (Milwaukee, WI). All reagents and chemicals were ACS grade or better and were used without further purification.

The peptides were assembled on pMBHA resin (0.28 mequiv/g substitution) purchased from Peptides International (Louisville, KY). The syntheses were performed using a 40-well Teflon reaction block with a coarse Teflon frit. Approximately 200 mg of resin (0.08 mmol) was added to each reaction block well. Each peptide was synthesized in two separate reaction wells because of reaction volume limitations. The resin was allowed to swell for 2 h in 5 mL of DMF, was deprotected using 4 mL of 50% TFA and 2% anisole in DCM for 3 min followed by a 20 min incubation at 500 rpms, and was washed with DCM (4.5 mL, 2 min, 500 rpm, three times). The peptide−resin salt was neutralized by the addition of 4 mL of 10% DIEA in DCM (3 min, 500 rpm, two times) followed by a DCM wash (4.5 mL, 2 min, 500 rpm, four times). A positive Kaiser[76] test resulted, indicating free amine groups on the resin. The growing peptide chain was added to the amide resin using the general amino acid cycle as follows: 500 μL of DMF is added to each reaction well to "wet the frit", a 3-fold excess of amino acid starting from the C-terminus is added [400 μM of 0.5 M solution in 0.5 M HOBt in DMF] followed by the addition of 400 μL of 0.5 M DIC in DMF, and the reaction well volume is brought up to 3 mL using DMF. The coupling reaction is mixed for 1 h at 500 rpms, followed by emptying of the reaction block by positive nitrogen gas pressure. A second coupling reaction is performed by the addition of 500 μL of DMF to each reaction vessel, followed by the addition of 400 μL of the respective amino acid (3-fold excess), 400 μL of 0.5 M HBTU, and 300 μL of 1 M DIEA. The reaction well volume is brought up to 3 mL with DMF and mixed at 500 rpm for 1 h. After the second coupling cycle, the reaction block is emptied and the resin-Nα-protected peptide is washed with DCM (4.5 mL, four times). Nα-Boc deprotection is performed by the addition of 4 mL of 50% TFA and 2% anisole in DCM and mixed for 5 min at 500 rpm followed by a 20 min deprotection. The reaction well is washed with 4.5 mL DCM (four times), neutralized with 10% DIEA (3 min, 500 rpm, two times) followed by a DCM wash (4.5 mL, 2 min, 500 rpm, four times), and the next coupling cycle is performed as described above. The Fmoc and OFm protecting groups are removed from Dpr and Asp, respectively, by treatment with 4.5 mL of 25% piperidine in DMF (20 min at 500 rpm), with a positive Kaiser test resulting. The lactam bridge between the Asp and Dpr amino acids is formed using a 5-fold excess of BOP and a 6-fold excess of DIEA as coupling agents and mixing at 500 rpms and monitored for cyclization completion by a negative Kaiser test. Deprotection of the remaining amino acid side chains and cleavage of the amide−peptide from the resin was performed by incubation the peptide−resin with anhydrous hydrogen fluoride (HF, 5 mL, 0 °C, 1 h) and 5% *m*-cresol and 5% thioanisole as scavengers. After the reaction is complete and the HF has been distilled off, the peptide is ether-precipitated (50 mL × 1) and washed with 50 mL of cold (4 °C) anhydrous ethyl ether. The peptide is filtered off using a coarse-frit glass filter, dissolved in glacial acetic acid, frozen, and lyophilized. The crude peptide yields ranged from 60% to 90% of the theoretical yields. A 40 mg sample of crude peptide was purified by RP-HPLC using a Shimadzu chromatography system with a photodiode array detector and a semipreparative reversed-phase high-performance liquid chromatography (RP-HPLC) C_{18} bonded silica column (Vydac 218TP1010, 1.0 cm × 25 cm) and lyophilized. The purified peptide was >95% pure as determined by analytical RP-HPLC and had the correct molecular mass (University of Florida Protein Core Facility) (Table 5).

Synthesis of Mini-AGRP and the Mini-(His-D-Phe-Arg-Trp)AGRP. The synthesis was performed using standard Fmoc methodology,[36,37] similar to that previously reported.[22,29,48] The Fmoc protected amino acids Cys(Acm), Cys(Trt), α-aminobutyric acid (Abu), Asp(tBu), Glu(tBu) Thr(tBu), Ser(tBu), Tyr(tBu), Arg(Pbf), Lys(tBu), His(Trt), Phe, Asn(Trt), Gln(Trt), Val, Gly, Pro, Ala, and Leu were purchased from Peptides International (Louisville, KY).

The peptides were assembled on Rink-amide-MBHA resin (0.4 mequiv/g substitution) purchased from Peptides International. The synthesis (0.3 mmol scale) was performed using a manual synthesis reaction vessel. Each synthetic cycle consisted of the following steps: (i) removal of the Nα Fmoc group by 20% piperidine in DMF (1 × 2 min, 1 × 20 min); (ii) single 2 h coupling of Fmoc-amino acid (3 equiv) using BOP (3 equiv), HOBt (3 equiv), and DIEA (6 equiv) in DMF and repeated until the peptide synthesis was complete. The presence or absence of the Nα free amino group was monitored using the Kaiser test.[76] After the completed synthesis, the peptides were cleaved from the resin and deprotected using a cleavage cocktail consisting of 82.5% TFA, 5% H_2O, 5% EDT, 5% phenol, and 2.5% TIS for 3 h at room temperature. After cleavage and side chain deprotection, the solution was concentrated and the peptide was precipitated and washed using cold (4 °C), anhydrous diethyl ether. The crude, linear peptides were

Table 5. Analytical Data for the Peptides Synthesized in This Study (Replaced Positions in Bold)[a]

peptide	structure	HPLC k' (system 1)	HPLC k' (system 2)	% purity	mass spectral analysis, m/z (M + 1)
1	Tyr-c[Asp-**Ala-Ala-Ala-**Asn-Ala-Phe-Dpr]-Tyr-NH_2	4.1	8.0	>99	1072.2
2	Tyr-c[Asp-**Arg-Phe-Phe-**Asn-Ala-Phe-Dpr]-Tyr-NH_2	6.0	9.0	>99	1310.5
3	Tyr-c[Asp-**Trp-Arg-Phe-**Asn-Ala-Phe-Dpr]-Tyr-NH_2	6.1	9.1	>98	1348.7
4	Tyr-c[Asp-**Trp-Arg-DPhe-**Asn-Ala-Phe-Dpr]-Tyr-NH_2	5.9	8.8	>99	1349.0
5	Tyr-c[Asp-**Phe-Arg-Trp-**Asn-Ala-Phe-Dpr]-Tyr-NH_2	6.1	9.1	>98	1347.7
6	Tyr-c[Asp-**DPhe-Arg-Trp-**Asn-Ala-Phe-Dpr]-Tyr-NH_2	5.8	8.5	>98	1348.3
7	Tyr-c[Asp-**His-Arg-Phe-Phe-**Asn-Ala-Phe-Dpr]-Tyr-NH_2	6.1	9.4	>99	1445.8
8	Tyr-c[Asp-**His-Phe-Arg-Trp-**Asn-Ala-Phe-Dpr]-Tyr-NH_2	5.7	8.6	>99	1485.7
9	Tyr-c[Asp-**His-DPhe-Arg-Trp-**Asn-Ala-Phe-Dpr]-Tyr-NH_2	5.3	9.6	>99	1485.6
mini AGRP	Ac-hAGRP(87−120, Cys105Ala)-NH_2	6.2	11.4	>95	3939.6
	Ac-mini-**(His-DPhe-Arg-Trp)**hAGRP−NH_2	4.7	10.2	>95	4218.6

[a] HPLC k' = [(peptide retention time) − (solvent retention time)]/(solvent retention time) in solvent system 1 (10% acetonitrile in 0.1% trifluoroacetic acid/water and a gradient to 90% acetonitrile over 35 min) and solvent system 2 (10% methanol in 0.1% trifluoroacetic acid/water and a gradient to 90% methanol over 35 min). An analytical Vydac C18 column (Vydac 218TP104) was used with a flow rate of 1.5 mL/min. The peptide purity was determined by HPLC at a wavelength of 214 nm.

purified by reversed-phase HPLC using a Shimadzu chromatography system with a photodiode array detector and a semipreparative RP-HPLC C_{18} bonded silica column (Vydac 218TP1010, 1.0 cm × 25 cm). Disulfide cyclization was performed in solution by dissolving 10 mg of purified linear peptide in 5 mL of DMSO and adding it to the oxidation buffer (0.01 M Tris, 0.2 M guanidine hydrochloride, 0.2 mM oxidized glutathione, and 1 mM reduced glutathione in water) and mixing at room temperature until cyclization was complete (30 min to 2 h, monitored by RP-HPLC). The oxidized peptide solution was acidified to pH 3 with 100% TFA and purified by RP-HPLC. The purified peptides were at least >95% pure as determined by RP-HPLC in two diverse solvent systems and had the correct molecular mass (University of Florida Protein Core Facility) (Table 5).

Cell Culture and Transfection. Briefly, HEK-293 cells were maintained in Dulbecco's modified Eagle's medium (DMEM) with 10% fetal calf serum and seeded 1 day prior to transfection at (1−2) × 10^6 cells per 100 mm dish. Melanocortin receptor DNA in the $pCDNA_3$ expression vector (20 μg) was transfected using the calcium phosphate method. Stable receptor populations were generated using G418 selection (1 mg/mL) for subsequent bioassay analysis.

Functional cAMP Based Bioassay. HEK-293 cells stably expressing the melanocortin receptors were transfected with 4 μg of CRE/β-galactosidase reporter gene as previously described.[20,41,60] Briefly, 5000−15000 posttransfection cells were plated into 96-well Primera plates (Falcon) and incubated overnight. Forty-eight hours posttransfection, the cells were stimulated with 100 μL of peptide (10^{-4}−10^{-12} M) or forskolin (10^{-4} M) control in assay medium (DMEM containing 0.1 mg/mL BSA and 0.1 mM isobutylmethylxanthine) for 6 h. The assay media was aspirated, and 50 μL of lysis buffer (250 mM Tris-HCl, pH 8.0, and 0.1% Triton X-100) was added. The plates were stored at −80 °C overnight. The plates containing the cell lysates were thawed the following day. Aliquots of 10 μL were taken from each well and transferred to another 96-well plate for relative protein determination. To the cell lysate plates, 40 μL of phosphate-buffered saline with 0.5% BSA was added to each well. Subsequently, 150 μL of substrate buffer (60 mM sodium phosphate, 1 mM $MgCl_2$, 10 mM KCl, 5 mM β-mercaptoethanol, 200 mg/100 mL ONPG) was added to each well and the plates were incubated at 37 °C. The sample absorbance, OD_{405}, was measured using a 96-well plate reader (Molecular Devices). The relative protein was determined by adding 200 μL of 1:5 dilution Bio Rad G250 protein dye/water to the 10 μL cell lysate sample taken previously, and the OD_{595} was measured on a 96-well plate reader (Molecular Devices). Data points were normalized to both the relative protein content and the nonreceptor-dependent forskolin stimulation. The antagonistic properties of these compounds were evaluated by the ability of these ligands to competitively displace the MTII agonist (Bachem) in a dose-dependent manner, at up to 10 μM concentrations.[20] The pA_2 values were generated using the Schild analysis method.[77]

Data Analysis. EC_{50} and pA_2 values represent the mean of duplicate experiments performed in triplet, quadruplet, or more independent experiments. EC_{50} and pA_2 estimates, and their associated standard errors, were determined by fitting the data to a nonlinear least-squares analysis using the PRISM program (version 4.0, GraphPad Inc.).

Binding Assays. NDP-MSH and hAGRP(87−132) Iodination. [^{125}I]-NDP-MSH and [^{125}I]-AGRP(87−132) were prepared using a modified chloramine T method as previously described by Yang et al.[54] By use of 50 mM sodium phosphate buffer, pH 7.4, as the reaction buffer, [^{125}I]-Na (0.5 mCi, Amersham Life Sciences, Inc., Arlington Heights, IL) was added to 20 μg of NDP-MSH (Bachem, Torrance, CA) or 20 μg of AGRP(87−132) (Peptides International, Louisville, KY) in 5 μL of buffer. To initiate the reaction, 10 μL of a 2.4 mg/mL solution of chloramine T (Sigma Chemical Co., St. Louis, MO) was added for 15 s with gentle agitation. This reaction was terminated by the addition of 50 μL of a 4.8 mg/mL solution of sodium metabisulfite (Sigma Chemical Co.) for 20 s with gentle agitation. The reaction mixture was then diluted with 200 μL of 10% bovine serum albumin, and the resultant mixture was layered on a Bio-Gel P2 (Bio-Rad Labs, Hercules, CA) column (1.0 cm × 30 cm Econocolumn, Bio-Rad Labs) for NDP-MSH or on a Bio-Gel P6 (Bio-Rad labs, Hercules, CA) column (1.0 cm × 50 cm Econocolumn, Bio-Rad Labs) for AGRP(87−132) for separation by size exclusion chromatography using 50 mM sodium phosphate buffer, pH 7.4, as column eluant. Fifteen drop fractions (approximately 500 μL) were collected into glass tubes containing 500 μL of 1% BSA. Each fraction was then counted on the Apex Automatic Gamma Counter (ICN Micromedic Systems, model 28023, Huntsville, AL, with RIA AID software, Robert Maciel Associates, Inc., Arlington, MA) to determine peak ^{125}I incorporation fractions.

Receptor Binding Studies. HEK-293 cells stably expressing the melanocortin receptors were maintained as described above. One day preceding the experiment, 0.3 × 10^6 cells/well were plated into Primera 24-well plates (Falcon). The NDP-MSH, hAGRP(87−132), and peptides being examined were used to competitively displace the ^{125}I-radiolabeled NDP-MSH or hAGRP(87−132) (100 000 cpm/well) in a dose−response (10^{-5}−10^{-11} M) manner. A 450 μL solution of the peptide concentration being tested was added to the well. Next, a 50 μL solution of [^{125}I]-NDP-MSH or [^{125}I]-hAGRP(87−132) was added to each well, and the cells were incubated at 37 °C for 1 h. The medium was subsequently removed, and each well was washed with assay buffer (1 mL, DMEM, 0.1 mg/mL BSA). The cells were lysed by the addition of 0.5 mL of 0.1 M NaOH and 0.5 mL of 1% Triton X-100. The mixture was left to lyse the cells for 10 min, and the contents of each well were transferred to labeled 16 mm × 150 mm glass tubes and quantified using a Titertek 10 × 600 γ-counter (ICN Micromedic Systems, Huntsville, AL, with RIA AID software, Robert Maciel Associates, Inc., Arlington, MA). Dose−response curves and IC_{50} values were generated and analyzed by nonlinear least-squares analysis[78] and graphed using PRISM, version

4.0 (Graph pad). The IC_{50} values represent the mean of duplicate wells generated in at least two independent experiments, with the errors presented as the standard deviation of the mean.

Acknowledgment. This work has been supported by NIH Grants RO1-DK57080 and RO1-DK64250 (C.H.L.). Carrie Haskell-Luevano is a recipient of a Burroughs Wellcome Fund Career Award in the Biomedical Sciences and an American Diabetes Association Research Award. We thank Pilgrim Jackson and Glenn Millhauser at the University of California, Santa Cruz, CA, for their assistance and discussions regarding the mini-AGRP synthesis and folding.

Supporting Information Available: Amino acid sequence comparisons of rhodopsin and the melanocortin receptors of different species. This material is available free of charge via the Internet at http://pubs.acs.org.

References

(1) Ollmann, M. M.; Wilson, B. D.; Yang, Y.-K.; Kerns, J. A.; Chen, Y.; et al. Antagonism of Central Melanocortin Receptors in Vitro and in Vivo by Agouti-Related Protein. *Science* **1997**, *278*, 135−138.

(2) Huszar, D.; Lynch, C. A.; Fairchild-Huntress, V.; Dunmore, J. H.; Smith, F. J.; et al. Targeted Disruption of the Melanocortin-4 Receptor Results in Obesity in Mice. *Cell* **1997**, *88*, 131−141.

(3) Mountjoy, K. G.; Robbins, L. S.; Mortrud, M. T.; Cone, R. D. The Cloning of a Family of Genes That Encode the Melanocortin Receptors. *Science* **1992**, *257*, 1248−1251.

(4) Roselli-Rehfuss, L.; Mountjoy, K. G.; Robbins, L. S.; Mortrud, M. T.; Low, M. J.; et al. Identification of a Receptor for γ Melanotropin and Other Proopiomelanocortin Peptides in the Hypothalamus and Limbic System. *Proc. Natl. Acad. Sci. U.S.A.* **1993**, *90*, 8856−8860.

(5) Gantz, I.; Konda, Y.; Tashiro, T.; Shimoto, Y.; Miwa, H.; et al. Molecular Cloning of a Novel Melanocortin Receptor. *J. Biol. Chem.* **1993**, *268*, 8246−8250.

(6) Gantz, I.; Miwa, H.; Konda, Y.; Shimoto, Y.; Tashiro, T.; et al. Molecular Cloning, Expression, and Gene Localization of a Fourth Melanocortin Receptor. *J. Biol. Chem.* **1993**, *268*, 15174−15179.

(7) Gantz, I.; Shimoto, Y.; Konda, Y.; Miwa, H.; Dickinson, C. J.; et al. Molecular Cloning, Expression, and Characterization of a Fifth Melanocortin Receptor. *Biochem. Biophys. Res. Commun.* **1994**, *200*, 1214−1220.

(8) Chhajlani, V.; Muceniece, R.; Wikberg, J. E. S. Molecular Cloning of a Novel Human Melanocortin Receptor. *Biochem. Biophys. Res. Commun.* **1993**, *195*, 866−873.

(9) Chhajlani, V.; Wikberg, J. E. S. Molecular Cloning and Expression of the Human Melanocyte Stimulating Hormone Receptor cDNA. *FEBS Lett.* **1992**, *309*, 417−420.

(10) Pritchard, L. E.; Turnbull, A. V.; White, A. Pro-opiomelanocortin Processing in the Hypothalamus: Impact on Melanocortin Signalling and Obesity. *J. Endocrinol.* **2002**, *172*, 411−421.

(11) Lu, D.; Willard, D.; Patel, I. R.; Kadwell, S.; Overton, L.; et al. Agouti Protein Is an Antagonist of the Melanocyte-Stimulating-Hormone Receptor. *Nature* **1994**, *371*, 799−802.

(12) Gunn, T. M.; Miller, K. A.; He, L.; Hyman, R. W.; Davis, R. W.; et al. The Mouse Mahogany Locus Encodes a Transmembrane Form of Human Attractin. *Nature* **1999**, *398*, 152−156.

(13) Nagle, D. L.; McGrail, S. H.; Vitale, J.; Woolf, E. A.; Dussault, B. J., Jr.; et al. The Mahogany Protein Is a Receptor Involved in Suppression of Obesity. *Nature* **1999**, *398*, 148−152.

(14) He, L.; Gunn, T. M.; Bouley, D. M.; Lu, X. Y.; Watson, S. J.; et al. A Biochemical Function for Attractin in Agouti-Induced Pigmentation and Obesity. *Nat. Genet.* **2001**, *27*, 40−47.

(15) Reizes, O.; Lincecum, J.; Wang, Z.; Goldberger, O.; Huang, L.; et al. Transgenic Expression of Syndecan-1 Uncovers a Physiological Control of Feeding Behavior by Syndecan-3. *Cell* **2001**, *106*, 105−116.

(16) Nijenhuis, W. A.; Oosterom, J.; Adan, R. A. AGRP(83−132) Acts as an Inverse Agonist on the Human-Melanocortin-4 Receptor. *Mol. Endocrinol.* **2001**, *15*, 164−171.

(17) Haskell-Luevano, C.; Monck, E. K. Agouti-related Protein (AGRP) Functions as an Inverse Agonist at a Constitutively Active Brain Melanocortin-4 Receptor. *Regul. Pept.* **2001**, *99*, 1−7.

(18) Chai, B. X.; Neubig, R. R.; Millhauser, G. L.; Thompson, D. A.; Jackson, P. J.; et al. Inverse Agonist Activity of Agouti and Agouti-Related Protein. *Peptides* **2003**, *24*, 603−609.

(19) Bultman, S. J.; Michaud, E. J.; Woychick, R. P. Molecular Characterization of the Mouse Agouti Locus. *Cell* **1992**, *71*, 1195−1204.

(20) Haskell-Luevano, C.; Cone, R. D.; Monck, E. K.; Wan, Y.-P. Structure Activity Studies of the Melanocortin-4 Receptor by in Vitro Mutagenesis: Identification of Agouti-Related Protein (AGRP), Melanocortin Agonist and Synthetic Peptide Antagonist Interaction Determinants. *Biochemistry* **2001**, *40*, 6164−6179.

(21) Palczewski, K.; Kumasaka, T.; Hori, T.; Behnke, C. A.; Motoshima, H.; et al. Crystal Structure of Rhodopsin: A G Protein-Coupled Receptor. *Science* **2000**, *289*, 739−745.

(22) McNulty, J. C.; Thompson, D. A.; Bolin, K. A.; Wilken, J.; Barsh, G. S.; et al. High-Resolution NMR Structure of the Chemically-Synthesized Melanocortin Receptor Binding Domain AGRP(87−132) of the Agouti-Related Protein. *Biochemistry* **2001**, *40*, 15520−15527.

(23) Yang, Y.; Dickinson, C. J.; Zeng, Q.; Li, J. Y.; Thompson, D. A.; et al. Contribution of Melanocortin Receptor Exoloops to Agouti-Related Protein Binding. *J. Biol. Chem.* **1999**, *274*, 14100−14106.

(24) Yang, Y.; Chen, M.; Lai, Y.; Gantz, I.; Yagmurlu, A.; et al. Molecular Determination of Agouti-Related Protein Binding to Human Melanocortin-4 Receptor. *Mol. Pharmacol.* **2003**, *64*, 94−103.

(25) Haskell-Luevano, C.; Sawyer, T. K.; Trumpp-Kallmeyer, S.; Bikker, J.; Humblet, C.; et al. Three-Dimensional Molecular Models of the hMC1R Melanocortin Receptor: Complexes with Melanotropin Peptide Agonists. *Drug Des. Discovery* **1996**, *14*, 197−211.

(26) Yang, Y.-K.; Dickinson, C.; Haskell-Luevano, C.; Gantz, I. Molecular Basis for the Interaction of [Nle,^{4}DPhe^7] Melanocyte Stimulating Hormone with the Human Melanocortin-1 Receptor (Melanocyte α-MSH Receptor). *J. Biol. Chem.* **1997**, *272*, 23000−23010.

(27) Kiefer, L. L.; Veal, J. M.; Mountjoy, K. G.; Wilkison, W. O. Melanocortin Receptor Binding Determinants in the Agouti Protein. *Biochemistry* **1998**, *37*, 991−997.

(28) Yang, Y.; Fong, T. M.; Dickinson, C. J.; Mao, C.; Li, J. Y.; et al. Molecular Determinants of Ligand Binding to the Human Melanocortin-4 Receptor. *Biochemistry* **2000**, *39*, 14900−14911.

(29) Jackson, P. J.; McNulty, J. C.; Yang, Y. K.; Thompson, D. A.; Chai, B.; et al. Design, Pharmacology, and NMR Structure of a Minimized Cystine Knot with Agouti-Related Protein Activity. *Biochemistry* **2002**, *41*, 7565−7572.

(30) Nicholls, A.; Sharp, K. A.; Honig, B. Protein Folding and Association: Insights from the Interfacial and Thermodynamic Properties of Hydrocarbons. *Proteins* **1991**, *11*, 281−296.

(31) Holder, J. R.; Bauzo, R. M.; Xiang, Z.; Haskell-Luevano, C. Structure−Activity Relationships of the Melanocortin Tetrapeptide Ac-His-DPhe-Arg-Trp-NH_2 at the Mouse Melanocortin Receptors. Part 2. Modifications at the Phe Position. *J. Med. Chem.* **2002**, *45*, 3073−3081.

(32) Mergen, M.; Mergen, H.; Ozata, M.; Oner, R.; Oner, C. Rapid Communication: A Novel Melanocortin 4 Receptor (MC4R) Gene Mutation Associated with Morbid Obesity. *J. Clin. Endocrinol. Metab.* **2001**, *86*, 3448−3451.

(33) Haskell-Luevano, C. In Vitro Mutagenesis Studies of Melanocortin Receptor Coupling and Ligand Binding. *The Melanocortin Receptors*; The Humana Press Inc.: Totowa, NJ, 2000; pp 263−306.

(34) Lu, D.; Väge, D. I.; Cone, R. D. A Ligand-Mimetic Model for Constitutive Activation of the Melanocortin-1 Receptor. *Mol. Endocrinol.* **1998**, *12*, 592−604.

(35) Joseph, C. G.; Bauzo, R. M.; Xiang, Z.; Shaw, A. M.; Millard, W. J.; et al. Elongation Studies of the Human Agouti-Related Protein (AGRP) Core Decapeptide (Yc[CRFFNAFC]Y) Results in Antagonism at the Mouse Melanocortin-3 Receptor. *Peptides* **2003**, *27*, 263−270.

(36) Chang, C.; Meienhofer, J. Solid-Phase Peptide Synthesis Using Mild Base Cleavage of Nα-Fluorenylmethyloxycarbonyl Amino Acids, Exemplified by a Synthesis of Dihydrosomatostatin. *Int. J. Pept. Protein Res.* **1978**, *11*, 246−249.

(37) Carpino, L. A.; Han, G. Y. The 9-Fluorenylmethyloxycarbonyl Amino-Protecting Group. *J. Org. Chem.* **1972**, *37*, 3404−3409.

(38) Merrifield, R. B. Solid Phase Synthesis. II. The Syntheis of Bradykinin. *J. Am. Chem. Soc.* **1964**, *86*, 304−305.

(39) Tota, M. R.; Smith, T. S.; Mao, C.; MacNeil, T.; Mosley, R. T.; et al. Molecular Interaction of Agouti Protein and Agouti-Related Protein with Human Melanocortin Receptors. *Biochemistry* **1999**, *38*, 897−904.

(40) Haskell-Luevano, C.; Monck, E. K.; Wan, Y. P.; Schentrup, A. M. The Agouti-Related Protein Decapeptide (Yc[CRFFNAFC]Y) Possesses Agonist Activity at the Murine Melanocortin-1 Receptor. *Peptides* **2000**, *21*, 683−689.

(41) Chen, W.; Shields, T. S.; Stork, P. J. S.; Cone, R. D. A Colorimetric Assay for Measuring Activation of Gs- and Gq-Coupled Signaling Pathways. *Anal. Biochem.* **1995**, *226*, 349−354.

(42) Shutter, J. R.; Graham, M.; Kinsey, A. C.; Scully, S.; Lüthy, R.; et al. Hypothalamic Expression of ART, a Novel Gene Related to Agouti, Is Up-Regulated in Obese and Diabetic Mutant Mice. *Genes Dev.* **1997**, *11*, 593−602.
(43) Graham, M.; Shutter, J. R.; Sarmiento, U.; Sarosi, I.; Stark, K. L. Overexpression of AGRT Leads to Obesity in Transgenic Mice. *Nat. Genet.* **1997**, *17*, 273−274.
(44) Fan, W.; Boston, B. A.; Kesterson, R. A.; Hruby, V. J.; Cone, R. D. Role of Melanocortinergic Neurons in Feeding and the Agouti Obesity Syndrome. *Nature* **1997**, *385*, 165−168.
(45) Thirumoorthy, R.; Holder, J. R.; Bauzo, R. M.; Richards, N. G. J.; Edison, A. S.; et al. Novel Agouti-Related Protein (AGRP) Based Melanocortin-1 Receptor Antagonist. *J. Med. Chem.* **2001**, *44*, 4114−4124.
(46) Jarosinski, M. A.; Dodson, S. W.; Harding, B. J.; Hale, C.; McElvain, M.; et al. Design and Synthesis of Simplified AGRP-(65−112) Analogues: Protein-Mimetics with Affinity at the Melanocortin Receptors. Presented at the 2nd International and 17th American Peptide Symposium, San Diego, CA, June 9−14th, 2001; Poster 322.
(47) Arasasingham, P. N.; Fotsch, C.; Ouyang, X.; Norman, M. H.; Kelly, M. G.; et al. Structure−Activity Relationship of (1-Aryl-2-Piperazinylethyl)piperazines: Antagonists for the AGRP/Melanocortin Receptor Binding. *J. Med. Chem.* **2003**, *46*, 9−11.
(48) Bolin, K. A.; Anderson, D. J.; Trulson, J. A.; Thompson, D. A.; Wilken, J.; et al. NMR Structure of a Minimized Human Agouti Related Protein Prepared by Total Chemical Synthesis. *FEBS Lett.* **1999**, *451*, 125−131.
(49) Thompson, D. A.; Chai, B. X.; Rood, H. L.; Siani, M. A.; Douglas, N. R.; et al. Peptoid Mimics of Agouti Related Protein. *Bioorg. Med. Chem. Lett.* **2003**, *13*, 1409−1413.
(50) Joseph, C. G.; Bauzo, R. M.; Scott, J. W.; Haskell-Luevano, C. Stereochemical Inversion Studies of a Monocyclic hAGRP(103−122) Peptide. In *Peptide Revolution: Genomics, Proteomics & Therapeutics*, Proceedings of the 18th American Peptide Symposium; Kluwer Academic Publishers: Dordrecht, The Netherlands, in press.
(51) Wilczynski, A. M.; Bauzo, R. M.; Edison, A. S.; Thirumoorthy, R.; Haskell-Luevano, C. Structure and Function Studies of a Bicyclic Agouti-Related Protein (AGRP) Melanocortin-4 Receptor Antagonist. In *Peptide Revolution: Genomics, Proteomics & Therapeutics*, Proceedings of the 18th American Peptide Symposium; Kluwer Academic Publishers: Dordrecht, The Netherlands, in press.
(52) Wilson, K. R.; Wilczynski, A. M.; Scott, J. W.; Bauzo, R. M.; Haskell-Luevano, C. A Novel AGRP-Melanocortin Peptide Chimeric Library. In *Peptide Revolution: Genomics, Proteomics & Therapeutics*, Proceedings of the 18th American Peptide Symposium; Kluwer Academic Publishers: Dordrecht, The Netherlands, in press.
(53) Joseph, C. G.; Wilczynski, A. M.; Holder, J. R.; Bauzo, R. M.; Scott, J. W.; et al. Chimeric NDP-MSH and MTII Melanocortin Peptides with Agouti-Related Protein (AGRP) Arg-Phe-Phe Amino Acids Possess Agonist Melanocortin Receptor Activity. *Peptides*, in press.
(54) Yang, Y.-K.; Thompson, D. A.; Dickinson, C. J.; Wilken, J.; Barsh, G. S.; et al. Characterization of Agouti-Related Protein Binding to Melanocortin Receptors. *Mol. Endocrinol.* **1999**, *13*, 148−155.
(55) Unger, V. M.; Schertler, G. F. X. Low Resolution Structure of Bovine Rhodopsin Determined by Electron Cryo-microscopy. *Biophys. J.* **1995**, *68*, 1776−1786.
(56) Hruby, V. J.; Lu, D.; Sharma, S. D.; Castrucci, A. M. L.; Kesterson, R. A.; et al. Cyclic Lactam α-Melanotropin Analogues of Ac-Nle^4-c[Asp^5,D-Phe^7, Lys^{10}]-α-MSH(4−10)-NH_2 with Bulky Aromatic Amino Acids at Position 7 Show High Antagonist Potency and Selectivity at Specific Melanocortin Receptors. *J. Med. Chem.* **1995**, *38*, 3454−3461.
(57) Al-Obeidi, F.; Castrucci, A. M.; Hadley, M. E.; Hruby, V. J. Potent and Prolonged Acting Cyclic Lactam Analogues of α-Melanotropin: Design Based on Molecular Dynamics. *J. Med. Chem.* **1989**, *32*, 2555−2561.
(58) Sawyer, T. K.; Sanfillippo, P. J.; Hruby, V. J.; Engel, M. H.; Heward, C. B.; et al. 4-Norleucine, 7-D-Phenylalanine-α-Melanocyte-Stimulating Hormone: A Highly Potent α-Melanotropin with Ultra Long Biological Activity. *Proc. Natl. Acad. Sci. U.S.A.* **1980**, *77*, 5754−5758.
(59) Hruby, V. J.; Wilkes, B. C.; Cody, W. L.; Sawyer, T. K.; Hadley, M. E. Melanotropins: Structural, Conformational and Biological Considerations in the Development of Superpotent and Superprolonged Analogs. *Pept. Protein Rev.* **1984**, *3*, 1−64.
(60) Haskell-Luevano, C.; Holder, J. R.; Monck, E. K.; Bauzo, R. M. Characterization of Melanocortin NDP-MSH Agonist Peptide Fragments at the Mouse Central and Peripheral Melanocortin Receptors. *J. Med. Chem.* **2001**, *44*, 2247−2252.
(61) Butler, A. A.; Kesterson, R. A.; Khong, K.; Cullen, M. J.; Pelleymounter, M. A.; et al. A Unique Metabolic Syndrome Causes Obesity in the Melanocortin-3 Receptor-Deficient Mouse. *Endocrinology* **2000**, *141*, 3518−3521.
(62) Chen, A. S.; Marsh, D. J.; Trumbauer, M. E.; Frazier, E. G.; Guan, X. M.; et al. Inactivation of the Mouse Melanocortin-3 Receptor Results in Increased Fat Mass and Reduced Lean Body Mass. *Nat. Genet.* **2000**, *26*, 97−102.
(63) Baldwin, J. M.; Schertler, G. F. X.; Unger, V. An Alpha-Carbon Template for the Transmembrane Helices in the Rhodopsin Family of G-Protein Coupled Receptors. *J. Mol. Biol.* **1997**, *272*, 144−164.
(64) Thompson, J. D.; Higgins, D. G.; Gibson, T. J. CLUSTAL W: Improving the Sensitivity of Progressive Multiple Sequence Alignment through Sequence Weighting, Position-Specific Gap Penalties and Weight Matrix Choice. *Nucleic Acids Res.* **1994**, *22*, 4673−4680.
(65) Ballesteros, J. A.; Weinstein, H. Integrated Methods for the Construction of Three Dimensional Models and Computational Probing of Structure−Function Relations in G-Protein Coupled Receptors. *Methods Neurosci.* **1995**, *25*, 366−428.
(66) Garnier, J.; Gibrat, J. F.; Robson, B. GOR method for predicting protein secondary structure from amino acid sequence. *Methods Enzymol.* **1996**, *266*, 540−553.
(67) Brooks, B. R.; Bruccoleri, R. E.; Olafson, B. D.; States, D. J.; Swaminathan, S.; et al. CHARMM: A Program for Macromolecular Energy, Minimization, and Dynamics Calculations. *J. Comput. Chem.* **1983**, *4*, 187−217.
(68) MacKerell, A. D.; Brooks, B., Jr.; Brooks, C. L.; Nilsson, L., III; Roux, B.; et al. CHARMM: The Energy Function and Its Parameterization with an Overview of the Program. *The Encyclopedia of Computational Chemistry*; John Wiley & Sons: Chichester, U.K., 1998; pp 271−277.
(69) Sankararamakrishnan, R.; Konvicka, K.; Mehler, E. L.; H., W. Solvation in Simulated Annealing and High-Temperature Molecular Dynamics of Proteins: A Restrained Water Droplet Model. *Int. J. Quantum Chem.* **2000**, *77*, 174−186.
(70) Jorgensen, W. L.; Chandrasekhar, J.; Madura, J. D.; Impey, R. W.; Klein, M. L. Comparison of Simple Potential Functions for Simulating Liquid Water. *J. Chem. Phys.* **1983**, *79*, 926−935.
(71) Foloppe, N.; MacKerell, A. D. All-Atom Empirical Force Field for Nucleic Acids: 1. Parameter Optimization Based on Small Molecule and Condensed Phase Macromolecular Target Data. *J. Comput. Chem.* **2000**, *21*, 86−104.
(72) MacKerell, A. D.; Banavali, N. All-Atom Empirical Force Field for Nucleic Acids: 2. Application to Molecular Dynamics Simulations of DNA and RNA in Solution. *J. Comput. Chem.* **2000**, *21*, 105−120.
(73) MacKerell, A. D.; Bashford, D.; Bellott, M.; Dunbrack, R. L., Jr.; Evanseck, J. D.; et al. All-Atom Empirical Potential for Molecular Modeling and Dynamics Studies of Proteins. *J. Phys. Chem.* **1998**, *102*, 3586−3616.
(74) Van Gunsteren, W. F.; Berndsen, H. J. C. Algorithms for Macromolecular Dynamics and Constraint Dynamics. *J. Mol. Phys.* **1977**, *34*, 1311−1327.
(75) Stewart, J. M.; Young, J. D. *Solid Phase Peptide Synthesis*, 2nd ed.; Pierce Chemical Co.: Rockford, IL, 1984.
(76) Kaiser, E.; Colescott, R. L.; Bossinger, C. D.; Cook, P. I. Color Test for Detection of Free Terminal Amino Groups in the Solid-Phase Synthesis of Peptides. *Anal. Biochem.* **1970**, *34*, 595−598.
(77) Schild, H. O. pA, A New Scale for the Measurement of Drug Antagonism. *Br. J. Pharmacol.* **1947**, *2*, 189−206.
(78) Bowen, W. P.; Jerman, J. C. Nonlinear Regression Using Spreadsheets. *TIPS* **1995**, *16*, 413−417.

JM0303608